Visual Neuroscience (2002), **19**, 735–753. Printed in the USA.

DOI: 10.1017/S0952523802196052

A simple model accounts for the response of disparity-tuned V1 neurons to anticorrelated images

JENNY C.A. READ,[1,2] ANDREW J. PARKER,[1] AND BRUCE G. CUMMING[1,2]

[1]University Laboratory of Physiology, Oxford University, Parks Road, Oxford
[2]Laboratory of Sensorimotor Research, National Eye Institute, National Institutes of Health, Bethesda

(RECEIVED March 19, 2002; ACCEPTED October 9, 2002)

Abstract

Disparity-tuned cells in primary visual cortex (V1) are thought to play a significant role in the processing of stereoscopic depth. The disparity-specific responses of these neurons have been previously described by an energy model based on local, feedforward interactions. This model fails to predict the response to binocularly anticorrelated stimuli, in which images presented to left and right eyes have opposite contrasts. The original energy model predicts that anticorrelation should invert the disparity tuning curve (phase difference π), with no change in the amplitude of the response. Experimentally, the amplitude tends to be reduced with anticorrelated stimuli and a spread of phase differences is observed, although phase differences near π are the most common. These experimental observations could potentially reflect a modulation of the V1 signals by feedback from higher visual areas (because anticorrelated stimuli create a weaker or nonexistent stereoscopic depth sensation). This hypothesis could explain the effects on amplitude, but the spread of phase differences is harder to understand. Here, we demonstrate that changes in both amplitude and phase can be explained by a straightforward modification of the energy model that involves only local processing. Input from each eye is passed through a monocular simple cell, incorporating a threshold, before being combined at a binocular simple cell that feeds into the energy computation. Since this local feedforward model can explain the responses of complex cells to both correlated and anticorrelated stimuli, there is no need to invoke any influence of global stereoscopic matching.

Keywords: Binocular disparity, Stereo correspondence, Visual cortex, Complex cells, Depth perception

Introduction

Many aspects of the behavior of disparity-tuned neurons in V1 (Barlow et al., 1967; Nikara et al., 1968; Poggio & Fischer, 1977) are captured by the "energy model" proposed by Adelson and Bergen (1985) for motion, and adapted for stereopsis by Ohzawa et al. (1990, 1997). In this model, the responses of complex cells can be separated into two terms: one that depends only on the contrast energy presented to each eye and another that depends on the relationship between images in the two eyes. The latter term varies with the stimulus disparity. This model describes satisfactorily both the binocular response profile obtained with disparate bar stimuli and the disparity tuning curve obtained by averaging the response to many different random-dot stimuli with a given disparity (reviewed by Cumming & DeAngelis, 2001).

Cumming and Parker (1997) showed that the energy model fails when V1 neurons are probed with binocularly anticorrelated stimuli, in which the contrast in one eye is inverted with respect to the other (black pixels are replaced with white and *vice versa*, see Fig. 1). With the energy model, the disparity-modulated term simply changes sign when the stimuli are binocularly anticorrelated. Thus, disparity tuning curves obtained with anticorrelated random-dot stimuli (RDS) should always have the same amplitude as those obtained with correlated stimuli, and differ by π in their phase. This is not observed experimentally. The amplitude of the modulation is usually smaller for anticorrelated stimuli (in extreme cases, there is no modulation, e.g. Fig. 5) and there are phase differences significantly different from π (Cumming & Parker, 1997). Equivalent phenomena can be identified in earlier studies with bar stimuli (Ohzawa et al., 1990, 1997). The purpose of this paper is to examine whether a straightforward modification of the energy model can be developed to account for these phenomena.

The experimental observations also have implications for the role of V1 complex cells in stereoscopic depth perception. To extract stereoscopic depth from retinal disparity, the visual system must correctly match each point on the left retina with its partner in the right. This *correspondence problem* is especially apparent in RDS, where there are many false targets to confound a local matching algorithm. The interesting feature of binocular anticorrelation is that it completely prevents the achievement of a global solution with dense random-dot stimuli (Julesz, 1971; Cogan et al.,

Address correspondence and reprint requests to: Jenny C.A. Read, Laboratory of Sensorimotor Research, National Eye Institute, National Institutes of Health, 49 Convent Drive, Bethesda, MD 20892-4435, USA.

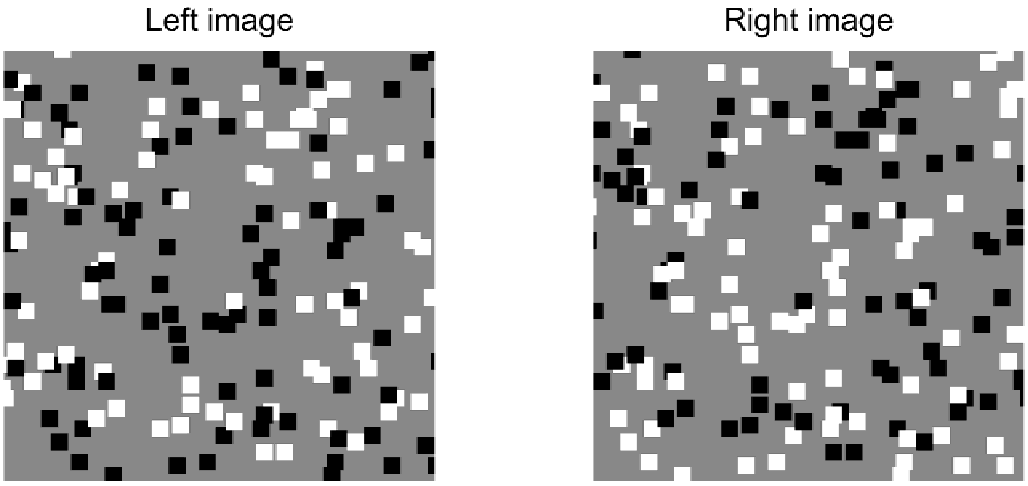

Fig. 1. Anticorrelated random-dot pattern. The figure shows a pair of disparate images. The contrast in the right eye's image is inverted relative to the left eye, so that white dots in the left eye are black in the right eye, and *vice versa*. The disparity between this pair of images is 6 pixels; the dot-size is 5 pixels.

1995; Cumming et al., 1998; Read & Eagle, 2000). Yet V1 neurons modulate their response as a function of disparity with the same stimuli that fail to provide a consistent perception of depth (Cumming & Parker, 1997; Cumming et al., 1998). Arguably, then, disparity-tuned V1 neurons must be a stage some way removed from the perception of stereoscopic depth.

On the other hand, the weaker amplitude of the response to anticorrelation might suggest that V1 neurons are sensitive to the global solution of the correspondence problem (Ohzawa, 1998). This could be the result of feedback from higher visual areas encoding the global solution, which suppress responses in V1 to stimuli for which no solution is found. In this paper, we search for a satisfactory local model that can account for the observed behavior of V1 complex cells to bar and random-dot stereograms. Such a model would repair this deficiency of the energy model, and obviate the need to invoke higher level feedback to V1 to explain these phenomena.

Materials and methods

Numerical simulations were written in MATLAB. In each case, the model retina was 128×128 pixels. The random-dot patterns (e.g. Fig. 1) had dot size 5 pixels and dot density 25%, meaning that if none of the dots overlapped, they would occupy 25% of the image. In numerical simulations using random-dot patterns (Figs. 2, 4, 8, 10, & 13), the results shown are the mean response to 5000 stimuli at each disparity (500,000 for Fig. 12). The curves joining the dots are obtained by spline interpolation. For comparison, the mean response to uncorrelated images is indicated with horizontal lines (marked "U").

When the model was used with Gabor receptive fields (Figs. 2, 4, 8, & 12), the spatial period of the Gabor was 64 pixels, the spatial-frequency bandwidth 2.5 octaves, and the orientation bandwidth 30 deg (both defined as the full width at half-maximum of the tuning curve obtained with monocular sine-grating stimuli). This implies a Gaussian envelope with standard deviations of 12 and 32 pixels, respectively, orthogonal and parallel to the carrier sinusoid. The same size of envelope was used when the model was tested with Gaussian receptive fields (Fig. 10).

Results

Overview

1. We first describe the energy model of Ohzawa et al. (1990), and show why it predicts response modulations of equal amplitude for correlated and anti-correlated stereograms.
2. An output nonlinearity can produce amplitude ratios less than one for cells with even-symmetric disparity tuning curves, but this requires different nonlinearities for tuned excitatory (TE) cells and tuned inhibitory (TI) cells.
3. Half-wave rectification of the monocular inputs, prior to binocular combination, produces amplitude ratios less than one for TE-type even-symmetric tuning curves. This could be implemented by binocular simple (BS) cells receiving excitatory input from monocular simple cells.
4. Neither of these methods can produce odd-symmetric responses with amplitude ratios less than one.
5. We show two sources of odd-symmetry in the energy model. First, when an even-symmetric receptive field (RF) in one eye is paired with an odd-symmetric RF in the other, the disparity tuning curve will be odd symmetric. Second, if the response is inverted by exchanging the left and right images (*LR* interchange antisymmetry), the disparity tuning curve must be odd symmetric. Both of these factors independently guarantee odd symmetry in the implementation of Ohzawa et al. (1990).
6. Our modified BS cells can be used to implement *LR* interchange antisymmetry by combining excitatory inputs from one eye (after rectification) with suppressive input from the other (passed through an inhibitory synapse after rectification). This produces TI and odd-symmetric disparity tuning curves with amplitude ratios less than one.
7. When tested with drifting gratings of different disparities, the temporal modulation in the response of modified BS cells receiving purely excitatory input from each eye shows a

distinctive pattern. At some disparities, they show strong modulation at the second harmonic of the stimulus frequency. This feature could be eliminated by an output threshold at the final stage. Nonetheless, we report several examples of simple cells from primate V1 that show exactly this pattern of modulation.

Properties of binocular complex cells

Many disparity tuning curves of V1 neurons are well fitted by Gabor functions of the general form (Ohzawa et al., 1997; Anzai et al., 1999*a*,*b*; Prince et al., 2002*a*)

$$f(\delta) = A\exp[-(\delta-\delta_0)^2/(2\sigma^2)]\cos[2\pi\omega(\delta-\delta_0)+\phi]+U. \quad (1)$$

A, ω, and ϕ are, respectively, the amplitude, spatial frequency, and phase of the carrier sinusoid, σ is the standard deviation of the Gaussian envelope, U is the firing rate to binocularly uncorrelated stimuli, and δ_0 is a disparity offset (the disparity δ at which the Gaussian envelope is largest).

Cumming and Parker (1997) quantified the effect of binocular anticorrelation by using nonlinear regression to fit a linked pair of Gabor functions to both the correlated and the anticorrelated data [eqn. (1)]. The disparity offset, baseline firing rate, spatial frequency, and bandwidth of the two Gabor functions were constrained to be the same for both sets of data, but different values of the amplitude A and phase ϕ were permitted. They then calculated the ratio of the amplitudes fitted to the correlated and anticorrelated data: A_a/A_c. According to the energy model, this amplitude ratio should be unity (Fig. 2). Cumming and Parker found that, in the majority of cases, it was less than 1 and sometimes as small as 0.01.

We therefore begin by looking again at the energy model, which we develop in more general terms than usual, in order to bring out those features of the model that cause it to show an amplitude ratio of 1 and to see how these features might be modified.

Model simple cells

The energy model is based on simple cells that exhibit linear spatial summation followed by an output nonlinearity (Hubel & Wiesel, 1962; Movshon et al., 1978; Anzai et al., 1999*b*). The response of simple cells can be characterized with a RF function $\rho(x,y)$, which represents the level of excitation caused by a spot of light at position (x,y) in the retina. Positive values of $\rho(x,y)$ correspond to an ON region of the RF, in which bright stimuli cause the cell to increase its firing, and negative values to an OFF region, in which bright stimuli suppress firing and dark stimuli increase it. We represent the retinal image by the function $I(x,y)$, which is the contrast between the luminance at retinal position (x,y) and the mean luminance averaged across the whole image. Thus positive values of $I(x,y)$ represent bright features, while negative values represent dark features. The response of a purely linear simple cell would be simply the inner product of the image with the RF function:

$$v = \iint \mathrm{d}x\,\mathrm{d}y\, I(x,y)\rho(x,y). \quad (2)$$

An array of such simple cells, with identical RFs situated at different positions across the retina, would encode the convolution of the image with the RF function. An individual simple cell signals the value of the convolution v at a single point.

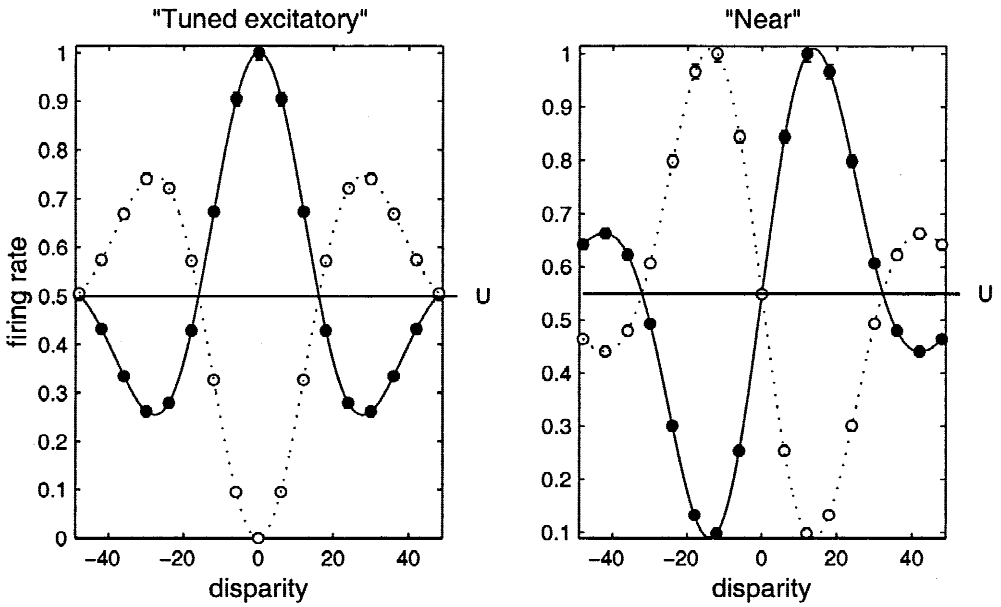

Fig. 2. Disparity tuning curves obtained with ODF model complex cells. The left-hand plot is for a "tuned excitatory"-type cell; the right-hand for a "near" cell. The filled dots and solid lines represent the response to correlated stereograms, while the empty dots and dotted lines that to anticorrelated stimuli; the horizontal line U shows the response to binocularly uncorrelated stimuli (these conventions are used in subsequent figures). Other details are as described in the Methods.

Notation

Many simple cells are binocular, with RFs in both eyes. In general, the images incident upon the two retinas are different. We distinguish left and right images with the labels L and R. Similarly, a BS cell has, in general, different RFs in each retina. Later notation will be streamlined if we use different labels to distinguish left and right RFs from those (L/R) used for images. We therefore use the labels s/*d* (*sinister*/*dexter*) to label the RFs in left and right retinas. Thus, the monocular convolutions are

$$v_L^{(s)} = \iint \mathrm{d}x\,\mathrm{d}y\, I_L(x,y)\rho^{(s)}(x,y),$$

$$v_R^{(d)} = \iint \mathrm{d}x\,\mathrm{d}y\, I_R(x,y)\rho^{(d)}(x,y). \tag{3}$$

Linear binocular combination

The energy model assumes that contributions from the left and right retinas, as well as contributions from different regions of the same retina, are summed linearly. Thus, the firing rate of the energy-model BS cell is not a general function of the convolutions in left and right eyes, $f(v_L^s, v_R^d)$, but actually a function only of their sum: $f(v_L^s + v_R^d)$. We refer to models with this property as showing linear binocular combination. Simple cells usually have low spontaneous firing rate so they cannot signal negative values. Their output is therefore the half-wave rectified sum of their inputs. Ohzawa et al. (1990, 1997) proposed that a BS cell incorporates an additional squaring nonlinearity, so that its output is the *square* of the half-wave rectified sum of left-eye and right-eye convolutions v_L and v_R:

$$S = [\mathrm{Pos}(v_L + v_R)]^2. \tag{4}$$

The energy model postulates that BS cells are combined in pairs, which we refer to as an ON cell and an OFF cell. Within each pair, the RFs in one simple cell are the inverses of those in the other simple cell, that is, an ON region of one cell corresponds to an OFF region in the other (Fig. 3), so that the convolutions have the opposite sign. Since $[\mathrm{Pos}(x)]^2 + [\mathrm{Pos}(-x)]^2 \equiv x^2$, the effect of combining pairs of ON/OFF cells in this way is to remove the half-wave rectification but leave the squaring nonlinearity:

$$S_{\mathrm{ON}} + S_{\mathrm{OFF}} = [v_L^{(s)} + v_R^{(d)}]^2 = [v_L^{(s)}]^2 + [v_R^{(d)}]^2 + 2v_L^{(s)}v_R^{(d)}. \tag{5}$$

Thus the total output of the pair of BS cells consists of left and right monocular terms, each depending only on one eye's image, and a cross-term, in which the left- and right-eye convolutions are multiplied together.

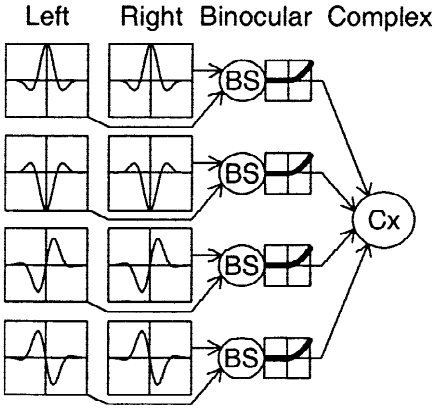

Fig. 3. Schematic diagram of the binocular energy model, based on the diagram in Fig. 3 of Ohzawa et al. (1990). The graphs show a cross section through the monocular RFs in left and right eyes. These feed into binocular simple cells ('BS'), which in turn feed into a complex cell ('Cx').

Responses to dynamic RDS and flashed bars

In this paper, we are mainly concerned with the results of experiments using dynamic RDS, such as those of Cumming and Parker (1997) or Poggio et al. (1985), in which the cell's response is averaged over many different image pairs that have the same disparity and degree of correlation. For images such as dynamic RDS, in which on average over time every point in the RF is exposed to the same luminance distribution, the average value of the monocular terms does not depend either on the disparity of the images or on their degree of correlation or anticorrelation. They form the constant component of the disparity tuning curve, representing the cell's response to binocularly uncorrelated images, U. The disparity-modulated component is given by the cross-term in eqn. (5). This cross-term makes no contribution to the average response to uncorrelated images, since it averages to zero over many uncorrelated image presentations. The squaring nonlinearity has effectively multiplied the left eye's input with the right eye's input, endowing the BS cell with its disparity tuning, which is then exploited by the complex neurons.

The Ohzawa-DeAngelis-Freeman (ODF) energy model (Ohzawa et al., 1990, 1997) combines input from two pairs of BS cells, with different RFs (Fig. 3):

$$C = S_{\mathrm{ON}}^{(1)} + S_{\mathrm{OFF}}^{(1)} + S_{\mathrm{ON}}^{(2)} + S_{\mathrm{OFF}}^{(2)} = [v_L^{(1s)}]^2 + [v_R^{(1d)}]^2 + [v_L^{(2s)}]^2 + [v_R^{(2d)}]^2 + 2[v_L^{(1s)}v_R^{(1d)} + v_L^{(2s)}v_R^{2d)}], \tag{6}$$

where, as before, the subscripts indicate whether the left (L) or right (R) image was used in the convolution, and the superscripts indicate which of four potentially different receptive fields $\rho^{(1s)}$, $\rho^{(1d)}$, $\rho^{(2s)}$, $\rho^{(2d)}$. The disparity-modulated component is given by the cross-terms:

$$D(\delta) = 2[v_L^{(1s)}v_R^{(1d)} + v_L^{(2s)}v_R^{(2d)}]. \tag{7}$$

The detailed behavior of this component depends on the choice of the four RF functions. In the original papers, Ohzawa et al. (1990, 1997) make various restrictions. They consider only RFs which are Gabor functions. They require the center, orientation, spatial period, and spatial extent of the Gabor to be the same in all four RFs, "to produce a sufficiently smooth binocular profile" (Ohzawa et al., 1997), and for each eye, they require a quadrature relationship between the RFs of the subunits (that is, $\rho^{(1s)}$ and $\rho^{(2s)}$ differ by $\pi/2$ in phase, as do $\rho^{(1d)}$ and $\rho^{(2d)}$).

The energy model fails because it is too linear

Regardless of these details, we can note certain properties any model of this form must possess. First, inverting the contrast of *both* eyes' images does not affect the cell's response, consistent with the experimentally measured behavior of examples of complex cells (Ohzawa et al., 1990, 1997). Second, eqn. (7) indicates that the disparity-modulated component D is inverted by anticorrelation. Each convolution is a linear function of the image, so the product of left and right convolutions changes sign without change of amplitude when the images become anticorrelated (Fig. 2). Thus, no model of this form can account for the attenuated response to anticorrelated stimuli. To achieve this, we need to introduce some sort of nonlinearity into the disparity-modulated term $D(\delta)$.

To understand what sort of nonlinearity might be necessary, we need to consider the range of disparity tuning curves displayed by real complex cells. As already discussed, these are generally well described by Gabor functions [eqn. (1)]. In our modeling work, it is convenient to begin by considering only tuning curves with zero disparity offset (i.e. $\delta_0 = 0$). This involves no loss of generality—it is trivial to obtain any desired δ_0 by shifting the monocular RFs. Similarly, we shall not be concerned with matching the baseline firing rate U to experimental data. In the results we present, the baseline firing rate may be larger, relative to the amplitude of the modulation, than typically observed. This could easily be adjusted by adding a final-stage output nonlinearity to the model complex cell, as in Fig. 4.

Experimentally, many different values of the tuning-curve phase ϕ are observed (Ohzawa et al., 1997; Anzai et al., 1999*c*; Prince et al., 2002*a*). Here, we concentrate on cells with $\phi = 0$ or π and $\phi = \pm\pi/2$. In the terminology of Poggio and Fischer (1977), cells with $\phi = 0$ would be classified as tuned excitatory (TE), cells with $\phi = \pi$ would be tuned inhibitory (TI), whereas those with $\phi = \pm\pi/2$ would be near or far cells (cf. Figs. 8 & 10). Cells with $\phi = 0$ or π have even symmetry about the central disparity δ_0, whereas cells with $\phi = \pm\pi/2$ have odd symmetry (cf. Fig. 2). That is (with $\delta_0 = 0$), even tuning curves have the symmetry $D(\delta) = D(-\delta)$ while odd curves have $D(\delta) = -D(-\delta)$. Restricting our attention to tuning curves that are purely odd or purely even does not involve a loss of generality, since any function can be expressed as a sum of an odd and an even component. Thus, if we can construct model complex cells which yield disparity tuning curves with $\phi = 0$ and $\phi = \pi/2$, then by suitably combining the inputs to these cells, we can obtain disparity tuning curves with any value of ϕ. It is helpful to make this restriction, because odd and even tuning curves present different problems. In particular, as we now demonstrate, modifications to the energy model that produce even disparity tuning curves with amplitude ratios of less than 1 do not necessarily have the same effect for odd tuning curves.

A single output nonlinearity can explain even- but not odd-symmetric tuning curves

An unsophisticated way of creating an even-symmetric disparity tuning curve (TE neuron) that shows an amplitude ratio less than 1 under anticorrelation is to superimpose an output nonlinearity on the standard ODF complex cell. Fig. 4 shows two examples. In the left-hand plot, the output nonlinearity is a threshold (Lippert & Wagner, 2001); in the right-hand plot, the response of the ODF cell has been squared. The effect of the nonlinearity in both cases is to enhance the response at high levels of excitation, relative to that at low excitation. This emphasizes the peak of the curve and weakens the side-flanks and troughs. Note that a different nonlinearity would be required to explain the reduced modulation in TI-type cells. Instead of a threshold, as for TE cells, we would have to postulate a saturation; instead of an expansive nonlinearity such as

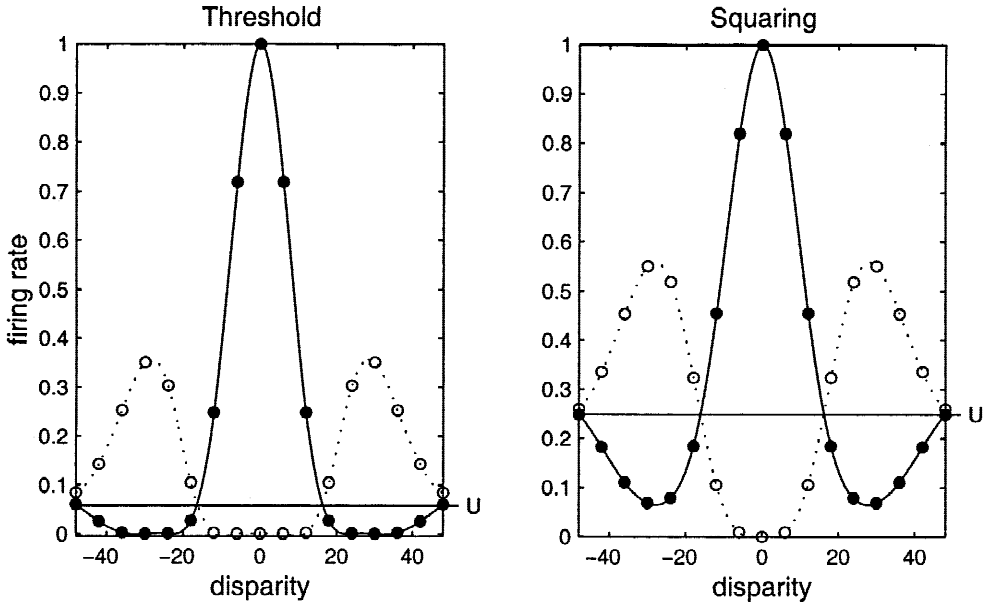

Fig. 4. The ODF model with an output nonlinearity. In the left-hand plot, the complex cell is given a threshold θ. If the output C of the ODF model exceeds θ, the cell fires at a rate $(C - \theta)$; if $C < \theta$, it is silent. In the right-hand plot, the cell fires at a rate C^2. The underlying simple cell RFs are Gabor functions in quadrature, shown in Fig. 9.

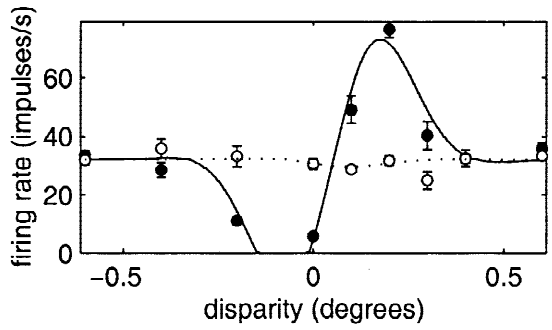

Fig. 5. Experimental data from a complex cell with an odd-symmetric disparity tuning curve. Experimental details as in Cumming and Parker (1997). The curves show the Gabor fit. This cell shows strong disparity tuning for correlated stimuli, and none at all for anticorrelated.

squaring, we would have to postulate a compressive nonlinearity such as square rooting. Such a model would therefore predict a systematic relationship between the shape of the disparity tuning curve and the nature of the nonlinearity. This prediction has not been tested experimentally but seems implausible. More significantly, a single output nonlinearity is incapable of constructing cells with odd-symmetric (near/far) disparity tuning curves which also show reduced amplitude under anticorrelation. The output nonlinearity necessarily has equal and opposite effects for crossed and uncrossed disparities, so that if it suppresses the modulation for anticorrelated stimuli at crossed disparities, it correspondingly boosts it at uncrossed disparities. Yet experimentally, there are clear examples of such cells (cf. the extreme example in Fig. 5). We asked what kind of model could, in principle, account for the response of these reduced-amplitude odd-symmetric cells.

General mechanisms for obtaining even and odd tuning curves

To understand the possible effects of anticorrelation in odd-symmetric cells, it is first vital to understand the properties of the model that give rise to the odd symmetry. In this section, therefore, we consider how to obtain complex cells with even and odd disparity tuning curves.

The ODF complex cell is built from pairs of ON/OFF BS cells. The disparity-modulated component of such a pair is simply the product of left- and right-eye convolutions, $(v_L^{(1s)} v_R^{(1d)})$. It can be shown (see Appendix A) that if the left- and right-eye RFs are both even, or both odd, about a particular point in the retina, then the product of left- and right-eye convolutions is, on average, unaffected by changing the sign of the disparity δ:

$$\langle v_L^{(s)} v_R^{(d)} \rangle(\delta) = \langle v_L^{(s)} v_R^{(d)} \rangle(-\delta). \tag{8}$$

That is, the sum of such an ON/OFF pair of BS cells yields an even tuning curve. (To be precise, the tuning curve is even about zero only if the left/right RFs are symmetric about binocularly corresponding points in the left and right retinas; otherwise, the tuning curve is symmetric about a disparity δ_0 corresponding to the position disparity between the centers of symmetry in each retina). Conversely, if the RF in one eye is odd and the other even, a pair of ON/OFF BS cells yields an odd tuning curve (Appendix A; Ohzawa et al., 1990). This result does not depend on the precise form of the RFs, merely on their symmetry about an arbitrary point in the retina. The most general monocular RF can always be expressed as the sum of an even and an odd component. The resulting disparity tuning curve has a phase that depends on the relative weighting of odd and even components in each eye.

The problem is that the initial linear stage of the ODF model guarantees that responses of odd-symmetric tuning curves will show the same degree of modulation for both correlated and anticorrelated stimuli, in conflict with the experimental data. We therefore consider alternative, more general ways of obtaining even-symmetric and odd-symmetric tuning curves. The response of any model complex cell (C') must be a function of the left and right images: $C' = C'(I_L, I_R)$. The actual form of this function depends on the RFs in each eye. A sufficient—though not necessary—condition for a complex cell to yield an even disparity tuning curve is that its response to any stereogram remain the same when the disparity is inverted by exchanging the left and right images. Formally, to achieve even symmetry in this way, we require that the function $C'(I_L, I_R)$ must be symmetric under LR interchange—that is, unchanged when the labels L and R are swapped: $C'(I_L, I_R) = C'(I_R, I_L)$. Swapping the labels L and R corresponds to exchanging the left and right images, not the left and right RFs (which are indicated with the subscripts s/d).

One particular case of an LR-symmetric complex cell occurs when the left and right RF profiles are identical within all subunits ($\rho^{(1s)} = \rho^{(1d)}$, $\rho^{(2s)} = \rho^{(2d)}$). The even-symmetric complex cell of Ohzawa et al. (1990) (Fig. 2, left panel) has this property, meaning that it is actually even-symmetric twice over: it is symmetric under LR interchange *and* it is made from combining subunits with the same symmetry in both eyes. If there is more than one subunit, a model with LR interchange symmetry is capable of delivering even-symmetric disparity tuning curves from complex cells even if the left and right RF profiles within each subunit differ in their symmetry properties. Referring back to eqn. (6), we see that if the left RF of the first subunit has the same profile as the right RF in the second subunit and *vice versa* (that is, $\rho^{(1s)} = \rho^{(2d)}$, $\rho^{(2s)} = \rho^{(1d)}$), then the response of the complex cell [eqn. (6)] can be written as

$$C = [v_L^{(1s)}]^2 + [v_R^{(1s)}]^2 + [v_L^{(2s)}]^2 + [v_R^{(2s)}]^2 + 2[v_L^{(1s)} v_R^{(1s)} + v_L^{(2s)} v_R^{(1s)}], \tag{9}$$

which is clearly unchanged when the labels L and R are swapped. Although models of this form produce even tuning curves, the curves can have a rather curious-looking shape that is not well described by a Gabor function (examples are shown in Figs. 8 and 10). Clearly, with more subunits still more possibilities would arise.

More pertinently, the same general approach can be followed to obtain odd disparity tuning curves. In order for the concept of odd tuning curve to make sense, we need to make one additional assumption about our general complex cell: that its response $C'(I_L, I_R)$ can be divided into a disparity-sensitive term $D'(I_L, I_R)$ and a disparity-independent term U representing the cell's response to binocularly uncorrelated images. Then, a sufficient (not necessary) condition for an odd tuning curve is that swapping the left and right images of an arbitrary stereogram changes the sign but not the amplitude of the disparity-modulated term. Formally, we require $D'(I_L, I_R) = -D'(I_R, I_L)$. We refer to a function with this property as being antisymmetric under LR interchange. An example of such a function is the model of Ohzawa et al. (1990)

with the RFs of the subunits related by $\rho^{(1s)} = \rho^{(2d)}$, $\rho^{(2s)} = -\rho^{(1d)}$. Then, eqn. (6) becomes

$$C = [v_L^{(1s)}]^2 + [v_R^{(2s)}]^2 + [v_L^{(2s)}]^2 + v_R^{(1s)}]^2 + 2[-v_L^{(1s)} v_R^{(2s)} + v_L^{(2s)} v_R^{(1s)}]. \quad (10)$$

The monocular, disparity-insensitive terms are clearly unaffected by swapping the labels L and R, while the disparity-sensitive cross-terms change sign. Thus the disparity tuning curve of this cell is odd. In the ODF model, eqn. (10) is used with $\rho^{(1s)}$ an even, and $\rho^{(2s)}$ an odd, Gabor function. Such a model is, again, odd symmetric twice over: it is antisymmetric under LR interchange, and also the individual disparity-modulated terms ($v_L^{(1s)} v_R^{(2s)}, v_L^{(2s)} v_R^{(1s)}$) are themselves odd. However, the LR interchange antisymmetry is, on its own, sufficient to yield an odd disparity tuning curve, whatever the RF profiles $\rho^{(1s)}$ and $\rho^{(2s)}$. The only requirement is that the subunits do not have identical RFs in the two eyes [in which case the disparity-selective terms in eqn. (10) cancel].

We note as an aside that the generation of odd-symmetric tuning curves does not require a Gabor-like RF structure incorporating ON and OFF regions. The fact that phase-disparity has often been employed within the original ODF model to yield odd-symmetric tuning curves risks giving the impression that phase-disparity is necessary for odd tuning curves, and thus that odd tuning curves provide evidence for phase-disparity. However, a counterexample is easy to construct. Imagine two tuned-excitatory complex cells like those in Ohzawa et al. (1990), with different position disparities ensuring that they are tuned to different disparities. Now consider a cell which receives excitatory input from one and inhibitory input from the other. Clearly this will have an odd-symmetric tuning curve, although for each binocular subunit, the phase-disparity is zero.

A new model: Monocular simple cells prior to binocular combination

We have seen that in order to obtain an attenuated response to anticorrelated stimuli within the basic framework of the original ODF model, we must add a nonlinearity to the binocular simple cell. Out of many potential choices for such a nonlinearity, one which seems particularly straightforward and biologically plausible is the case where input from the retinal RFs passes first to a monocular simple cell rather than feeding directly onto a BS cell. BS cells would then receive input from two monocular simple cells, as sketched in Fig. 6. The effect of this is that the monocular convolutions [eqn. (3)] from the two eyes are half-wave rectified *before* being combined. That is, the firing rate of each BS cell is now given by

$$S' = [\mathrm{Pos}(v_L) + \mathrm{Pos}(v_R)]^2. \quad (11)$$

[cf. eqn. (4)].

For simplicity, we have assumed that the monocular simple cells implement only half-wave rectification. In fact, we have found that qualitatively similar results are obtained if, like the model BS cells, they also include a squaring nonlinearity. The key features of our model do not depend on the precise form of the point nonlinearity prior to binocular combination. Similarly, although it seems natural to interpret our model in terms of a hierarchy, in which monocular simple cells feed into BS cells, this is not formally required. We could equally envisage the BS cell [eqn. (11)] as receiving input directly from the lateral geniculate nucleus (LGN), with the half-wave rectification implemented at the synaptic or dendritic level.

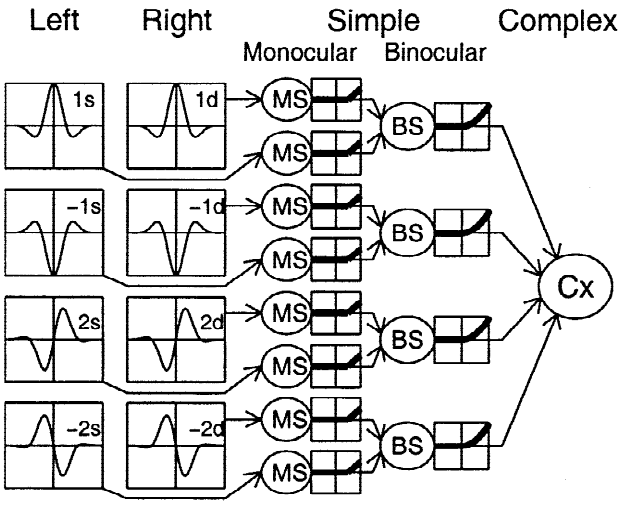

Fig. 6. Schematic diagram of our new model. Input from the retinal RFs is not fed directly to BS cells, but is passed *via* monocular simple cells ('MS'). This introduces a rectifying nonlinearity prior to binocular combination. In this paper, the computational results are from a model in which monocular simple cells signal the sum of their inputs provided this exceeds a threshold. Initially we set this threshold at zero, that is, half-wave rectification; in later results we raise the threshold above zero. Qualitatively similar results are obtained if the output of the monocular simple cells is a threshold followed by a squaring nonlinearity, as for the binocular simple cells ('BS'). The circuitry shown in this figure produces TE-type disparity tuning curves; analogous circuitry which produces near/far tuning curves is shown in Fig. 7.

As in the ODF model, we construct a complex cell which receives input from four such simple cells, two pairs of matching ON/OFF cells:

$$S'^{(1)}_{\mathrm{ON}} = [\mathrm{Pos}(v_L^{(1s)}) + \mathrm{Pos}(v_R^{(1d)})]^2$$
$$S'^{(1)}_{\mathrm{OFF}} = [\mathrm{Pos}(-v_L^{(1s)}) + \mathrm{Pos}(-v_R^{(1d)})]^2, \quad (12)$$

$$S'^{(2)}_{\mathrm{ON}} = [\mathrm{Pos}(v_L^{(2s)}) + \mathrm{Pos}(v_R^{(2d)})]^2,$$
$$S'^{(2)}_{\mathrm{OFF}} = [\mathrm{Pos}(-v_L^{(2s)}) + \mathrm{Pos}(-v_R^{(2d)})]^2. \quad (13)$$

The response of the complex cell is, again, given by the sum of the firing rates of the simple cells [eqn. (6)].

This is now equal to

$$C' = [v_L^{1s}]^2 + [v_R^{(1d)}]^2 + [v_L^{(2s)}]^2 + [v_R^{(2d)}]^2 + 2[\mathrm{Pos}(v_L^{(1s)})\mathrm{Pos}(v_R^{(1d)}) + \mathrm{Pos}(-v_L^{(1s)})\mathrm{Pos}(-v_R^{(1d)}) + \mathrm{Pos}(v_L^{(2s)}\mathrm{Pos}(v_R^{(2d)}) + \mathrm{Pos}(-v_L^{(2s)})\mathrm{Pos}(-v_R^{(2d)})]. \quad (14)$$

The monocular terms are the same as in the ODF energy model, but the cross-terms are half-wave rectified. As in the ODF model, the combination of ON and OFF simple cells ensures that the

response of our complex cell is unchanged by inverting the contrast in both eyes. Thus, the model responds equally well to binocularly presented bars regardless of whether they are both bright or both dark. Once again, we can divide the response of the complex cell into a component that arises from the four monocular terms and does not depend on disparity, and a component that is disparity modulated:

$$D'(\delta) = 2[\mathrm{Pos}(v_L^{(1s)})\mathrm{Pos}(v_R^{(1d)}) + \mathrm{Pos}(-v_L^{(1s)})\mathrm{Pos}(-v_R^{(1d)}) + \mathrm{Pos}(v_L^{(2s)})\mathrm{Pos}(v_R^{(2d)}) + \mathrm{Pos}(-v_L^{(2s)})\mathrm{Pos}(-v_R^{(2d)})] \quad (15)$$

[which may be compared with eqn. (7) for the ODF model].

The monocular half-wave rectification causes important differences in the behavior of the disparity-modulated term. For binocularly uncorrelated images, these cross-terms do *not* now average to zero. Thus, the response to uncorrelated images consists of a contribution from the four monocular terms in eqn. (14), as in the ODF model, *plus* a contribution from the disparity-modulated term. With correlated images, the contribution from the disparity-modulated term is suppressed at some disparities and enhanced at others. This is why a model of this form can produce disparity tuning curves which go below the uncorrelated level, even though the disparity-sensitive component in eqn. (15) is clearly never negative.

With this model, anticorrelation no longer simply inverts the tuning curve. Changing the sign of all the v_R in eqn. (15) does not simply change the sign of $D'(\delta)$ as it did in eqn. (7). Furthermore, we can see how this model might be capable of giving an attenuated response to anticorrelated stimuli. For instance, consider the situation where, for a particular correlated image pair, the convolutions $v_L^{(1s)}$ and $v_R^{(1d)}$ are both negative, while $v_L^{(2s)}$ and $v_R^{(2d)}$ are both positive. Then the disparity-modulated component is $D'_{corr} = 2[v_L^{(1s)}v_R^{(1d)} + v_L^{(2s)}v_R^{(2d)}]$. If we now invert the contrast of the right image, the response vanishes altogether: $D'_{\mathrm{anti}} = 0$.

This observation merely illustrates that it is possible for this model to generate weakened responses to anticorrelated stimuli. By itself, this observation does not guarantee that the amplitude of the tuning curve will actually be zero for anticorrelated stimuli, or even that it will be less than the amplitude for correlated stimuli. For instance, if the convolutions $v_L^{(1s)}$ and $v_R^{(1d)}$, and $v_L^{(2s)}$ and $v_R^{(2d)}$, have *opposite* sign, then the situation is reversed and this time $D'_{\mathrm{corr}} = 0$. The degree of attenuation for anticorrelated stimuli thus depends on how likely it is that the convolutions in the two eyes have the same sign when the stimuli are correlated. This in turn depends on the particular form of the RFs. As we shall demonstrate (Figs. 8, 10, & 12), plausible RFs can be chosen for which there is significant amplitude attenuation.

Generalizing to arbitrary tuning curves

It is easy to obtain a TE-type disparity tuning curve from the cell just developed. With the relations $\rho^{(1s)} = \rho^{(1d)}$, $\rho^{(2s)} = \rho^{(2d)}$ between the RF profiles in the different eyes, the disparity-modulated term in [eqn. (15)] becomes symmetric under LR interchange, and is thus even. Furthermore, for correlated stimuli its tuning curve peaks at zero disparity, since then the left and right images are identical and so $v_L^{(1s)} = v_R^{(1d)}$ $(= v^{(1)}$, say). This means that the disparity-modulated term [eqn. (15)] becomes $2[(v^{(1)})^2 + (v^{(2)})^2]$: that is, it is positive (not zero) for any image which drives the monocular simple cells at all, and so the complex cell's firing rate peaks. In contrast, for anticorrelated stimuli at zero disparity, the disparity-modulated term is always zero, meaning that the firing rate is minimum. Thus, this disparity tuning curve is of the TE type. It could be converted into a TI type merely by inverting the RF profiles in one eye, since the response previously obtained with anticorrelated stimuli would now be obtained with correlated stimuli. However, since the original cell is empirically found to have an amplitude ratio less than 1 (cf. Figs 8, 10, & 12), the TI-type tuning curve thus obtained would have an amplitude ratio of greater than 1.

To obtain TI-type and odd-symmetric tuning curves which show reduced amplitude to anticorrelated stimuli, we need to modify eqn. (15) by introducing minus signs. Although the mathematics is straightforward, the circuitry is slightly more complicated.

To implement a minus sign in eqn. (18), we must include simple cells that receive an excitatory input from one of the half-wave rectified monocular RFs but a subtractive inhibitory input from the other eye:

$$S' = \mathrm{Pos}[\mathrm{Pos}(v_L) - \mathrm{Pos}(v_R)]. \quad (16)$$

This possibility is automatically built into the ODF model, because their BS cells receive both excitatory and inhibitory influences from each retina. Thus if the convolution of the image with the RF is negative in one eye, it has a subtractive effect on the simple cell's firing rate. In our model, since we are half-wave rectifying the convolutions from each eye before they are combined, subtraction must be built in explicitly by using inhibitory interconnections. An additional overall half-wave rectification is included to prevent the model simple cell from having a negative firing rate. Once again we can effectively remove the half-wave rectification by combining BS cells in pairs: $[\mathrm{Pos}(x)]^2 + [\mathrm{Pos}(-x)]^2 \equiv x^2$. For instance, we can combine six BS cells to obtain a complex cell whose response is

$$\begin{aligned} C' = {} & [\mathrm{Pos}(v_L^{(1s)}) + \mathrm{Pos}(v_R^{(1d)})]^2 + [\mathrm{Pos}(-v_L^{(1s)}) + \mathrm{Pos}(-v_R^{(1d)})]^2 \\ & + \{\mathrm{Pos}[\mathrm{Pos}(v_L^{(2s)}) - \mathrm{Pos}(v_R^{(2d)})]\}^2 \\ & + \{\mathrm{Pos}[\mathrm{Pos}(-v_L^{(2s)}) - \mathrm{Pos}(-v_R^{(2d)})]\}^2 \\ & + \{\mathrm{Pos}[-\mathrm{Pos}(v_L^{(2s)}) + \mathrm{Pos}(v_R^{(2d)})]\}^2 \\ & + \{\mathrm{Pos}[-\mathrm{Pos}(-v_L^{(2s)}) + \mathrm{Pos}(-v_R^{(2d)})]\}^2. \end{aligned} \quad (17)$$

If we set $\rho^{(1s)} = \rho^{(2d)}$, and $\rho^{(2s)} = \rho^{(1d)}$, the disparity-modulated term is antisymmetric under LR interchange, and so the complex cell yields an odd disparity tuning curve. The circuitry is sketched in Fig. 7.

Thus, we have a family of models which is capable of giving disparity tuning curves of all four general types: TE/TI (even symmetry) and near/far (odd symmetry). We use complex cells whose output can be written as

$$\begin{aligned} C' = {} & [\mathrm{Pos}(v_L^{(1s)}) \pm \mathrm{Pos}(v_R^{(1d)})]^2 + [\mathrm{Pos}(-v_L^{(1s)}) \pm \mathrm{Pos}(-v_R^{(1d)})]^2 \\ & + [\mathrm{Pos}(v_L^{(2s)}) \pm \mathrm{Pos}(v_R^{(2d)})]^2 \\ & + [\mathrm{Pos}(-v_L^{(2s)}) \pm \mathrm{Pos}(-v_R^{(2d)})]^2. \end{aligned} \quad (18)$$

The pattern of the four plus and minus signs in this equation, together with the relationship between the RFs, determines the

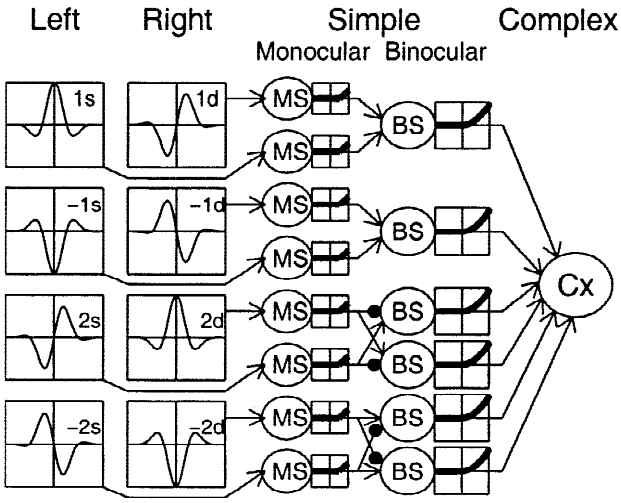

Fig. 7. Schematic diagram of our new model that produces odd disparity tuning curves in which the response to anticorrelated stimuli may be reduced. Although the example RFs in this figure have phase-disparity, this is not a prerequisite for odd disparity tuning curves. The solid dots represent inhibitory connections. The circuitry is slightly more complicated than the equivalent for TE-type tuning curves (Fig. 6), even though mathematically the difference between them is trivial. Briefly, the odd model involves the *difference* between positive quantities, whereas the even model involves the sum. Owing to the rectification at the simple cells, computing differences [using $(A - B) \equiv \mathrm{Pos}(A - B) + \mathrm{Pos}(B - A)$] requires twice as many cells as computing sums. To adapt this model for TI-type tuning curves, eight BS cells would be required, each receiving excitatory input from one eye and inhibitory input from the other.

type of tuning curve. If left and right RFs are identical ($\rho^{(1s)} = \rho^{(1d)}$, $\rho^{(2s)} = \rho^{(2d)}$), and all the signs are positive ($+ + + +$), eqn. (18) becomes the same as eqn. (14), representing a TE-type cell. With the same RF relations but all signs negative ($- - - -$), the disparity-modulated term is inverted, so we obtain a TI-type cell. With patterns $++--$ or $--++$, together with the relationships $\rho^{(1s)} = \rho^{(2d)}$ and $\rho^{(2s)} = \rho^{(1d)}$, the complex cell response is antisymmetric under LR interchange, and therefore yields an odd (near/far) disparity tuning curve.

However, if we combine the pattern $++++$ or $----$ with the RF relationship $\rho^{(1s)} = \rho^{(2d)}$ and $\rho^{(2s)} = \rho^{(1d)}$, we obtain a different type of even tuning curve, which is not well described by a Gabor function; it usually has a notch at the central disparity, flanked by side peaks. A few disparity tuning curves similar to this have been observed in the barn owl (Nieder & Wagner, 2000). Although they appear to be rare in the monkey (Prince et al., 2002*a*), it is possible that some examples have gone unrecognized because of limited sampling of the tuning curve in the experiments.

To generalize to disparity tuning curves incorporating a nonzero disparity offset δ_0, we simply have to shift the RFs in one eye by δ_0. To obtain tuning curves with intermediate phase ϕ, we can postulate a complex cell receiving input from multiple simple cells, some subgroups of which have the even-type connectivity (Fig. 6) and others the odd (Fig. 7).

To summarize, all our model complex cells include a disparity-independent component $[[v_L^{(1s)}]^2 + [v_R^{(1d)}]^2 + [v_L^{(2s)}]^2 + [v_R^{(2d)}]^2]$. The disparity-modulated component depends on the choice of pluses and minuses in eqn. (18), and on the relationships between the RF profiles. We highlight the following special cases:

- For TE/TI-type tuning curves which have even symmetry about the disparity δ_0:

$$D'_{\mathrm{even}}(\delta) = \pm 2[\mathrm{Pos}(v_L^{(1s)})\mathrm{Pos}(v_R^{(1d)}) + \mathrm{Pos}(-v_L^{(1s)})\mathrm{Pos}(-v_R^{(1d)}) + \mathrm{Pos}(v_L^{(2s)})\mathrm{Pos}(v_R^{(2d)}) + \mathrm{Pos}(-v_L^{(2s)})\mathrm{Pos}(-v_R^{(2d)})], \quad (19)$$

  with $\rho^{(1s)}(x, y) = \rho^{(1d)}(x + \delta_0, y)$, $\rho^{(2s)}(x, y) = \rho^{(2d)}(x + \delta_0, y)$; the $\pm$ controls whether the tuning is TE (+) or TI (−).
- For near/far-type tuning curves which have odd symmetry about the disparity δ_0:

$$D'_{\mathrm{odd}}(\delta) = \pm 2[\mathrm{Pos}(v_L^{(1s)})\mathrm{Pos}(v_R^{(1d)}) + \mathrm{Pos}(-v_L^{(1s)})\mathrm{Pos}(-v_R^{(1d)}) - \mathrm{Pos}(v_L^{(2s)})\mathrm{Pos}(v_R^{(2d)}) - \mathrm{Pos}(-v_L^{(2s)})\mathrm{Pos}(-v_R^{(2d)})], \quad (20)$$

  with $\rho^{(1s)}(x, y) = \rho^{(2d)}(x + \delta_0, y)$, $\rho^{(2s)}(x, y) = \rho^{(1d)}(x + \delta_0, y)$; the $\pm$ controls whether the tuning is near (+) or far (−).
- For tuning curves with a central notch which have even symmetry about the disparity δ_0:

$$D'_{\mathrm{even}}(\delta) = \pm 2[\mathrm{Pos}(v_L^{(1s)})\mathrm{Pos}(v_R^{(1d)}) + \mathrm{Pos}(-v_L^{(1s)})\mathrm{Pos}(-v_R^{(1d)}) + \mathrm{Pos}(v_L^{(2s)})\mathrm{Pos}(v_R^{(2d)}) + \mathrm{Pos}(-v_L^{(2s)})\mathrm{Pos}(-v_R^{(2d)})], \quad (21)$$

  with $\rho^{(1s)}(x, y) = \rho^{(2d)}(x + \delta_0, y)$, $\rho^{(2s)}(x, y) = \rho^{(1d)}(x + \delta_0, y)$; the $\pm$ controls whether the side-flanks are positive or negative.

Simulation results

Having constructed our model complex cells, we performed numerical simulations to determine their responses to correlated and anticorrelated random-dot stereograms. Figs. 8 and 10 show the numerical simulations of all six types of tuning curve specified in eqns. (19)–(21) (with $\delta_0 = 0$) to illustrate the point that the new model shows an attenuated response to binocularly anticorrelated random-dot patterns. In Fig. 8, the underlying RFs (shown in Fig. 9) are Gabor functions like those employed by Ohzawa et al. (1990, 1997), differing in phase by $\pi/2$. In Fig. 10, the underlying RFs (Fig. 11) consist simply of a single Gaussian.

It is apparent in Figs. 8 and 10 that greater amplitude attenuation is obtained with the Gaussian RFs than with the Gabor. This reflects a general tendency, within our model, for amplitude ratios to be smaller when the RFs have large spatial-frequency bandwidth. In the limiting case where the RFs have infinitely narrow bandwidth, that is, are sinusoidal gratings of infinite extent, it can be shown that the amplitude of the disparity tuning curves is the same for correlated as for anticorrelated patterns (amplitude ratio 1), even for our modified version of the energy model. This means that Gabor RFs with obvious side-lobes rather than low-pass RFs tend to give amplitude ratios closer to 1, as exemplified in Figs. 8 and 10.

Note that, when Gabor RFs are used with the "notch" form of the model [eqn. (21)], the anticorrelated tuning curve is not

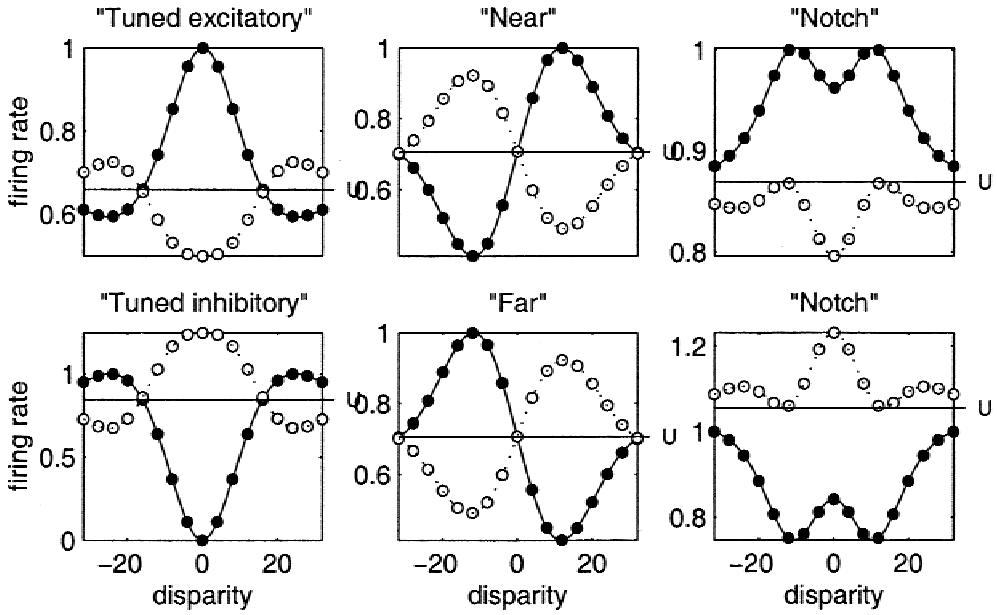

Fig. 8. Our new model with Gabor RFs (shown in Fig. 9). The six types of disparity tuning curves were obtained as explained in eqns. (19)–(21). For near/far-type tuning curves, only very slight attenuation is obtained with these RFs.

inverted. With the 1.5 octave bandwidth used here, it is virtually identical to the correlated tuning curves; with a broader bandwidth it would have smaller amplitude. The explanation for this, which depends on a detailed consideration of how the Gabor RF structure interacts with the anatomy of the notch model, requires more space than is warranted here, given that double-peaked cells are uncommon and their responses to binocular anticorrelation are unknown.

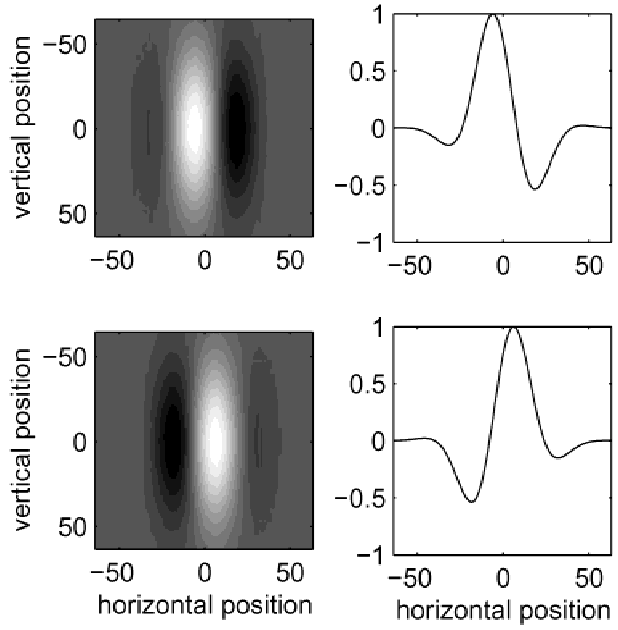

Fig. 9. Receptive fields used in obtaining the disparity tuning curves shown in Fig. 8. The left-hand images show the full RFs as a function of position in the retina. The plots on the right show a horizontal cross section through the RF profiles. In obtaining the TE/TI even tuning curves (left-most plots of Fig. 8), the upper RF profile was assigned to $\rho^{(1s)}$ and $\rho^{(1d)}$, and the lower to $\rho^{(2s)}$ and $\rho^{(2d)}$. In obtaining the odd and "notch" even tuning curves (middle- and right-most plots of Fig. 8), the upper RF profile was assigned to $\rho^{(1s)}$ and $\rho^{(2d)}$, and the lower to $\rho^{(2s)}$ and $\rho^{(1d)}$.

A higher threshold yields smaller amplitude ratios

With the model in the form developed so far [eqns. (19)–(21)], we have not been able to find RFs that yield amplitude ratios much smaller those shown in Figs. 8 and 10: around 0.5 or greater. Thus our model is not yet capable of matching the full range observed experimentally. Cumming and Parker (1997, Fig. 4) found a wide range of amplitude ratios, including a few greater than 1 (the cell responded better to anticorrelated than to correlated stimuli), and a few as low as 0.01 (there was hardly any response to anticorrelated stimuli). Our model is, of course, capable of producing amplitude ratios greater than 1, simply by changing the sign of all the right-eye convolutions in eqns. (19)–(21). To produce amplitude ratios below 0.5 and approaching zero, we must strengthen the half-wave rectification by raising the threshold: that is, we now assume that the monocular simple cells fire only if the net retinal input exceeds a threshold $\theta > 0$. Thus the response of the BS cell is

$$S_\theta = [\mathrm{Pos}(v_L - \theta) + \mathrm{Pos}(v_R - \theta)]^2. \tag{22}$$

We note that a similar threshold is also required in the ODF model [eqn. (4)] in order to produce the correct response to binocular drifting sinusoidal gratings. If the fundamental (F_1) harmonic component of the cell's response at the temporal frequency of the drifting grating is measured as a function of interocular phase, then the ODF model simple cell predicts that the magnitude of F_1 should be a constant fraction of the neuron's mean firing rate (F_0), regardless of the interocular phase. Experimentally, for many cells this ratio shows clear variation as a function of interocular phase. A threshold higher than zero is required to reproduce this variation

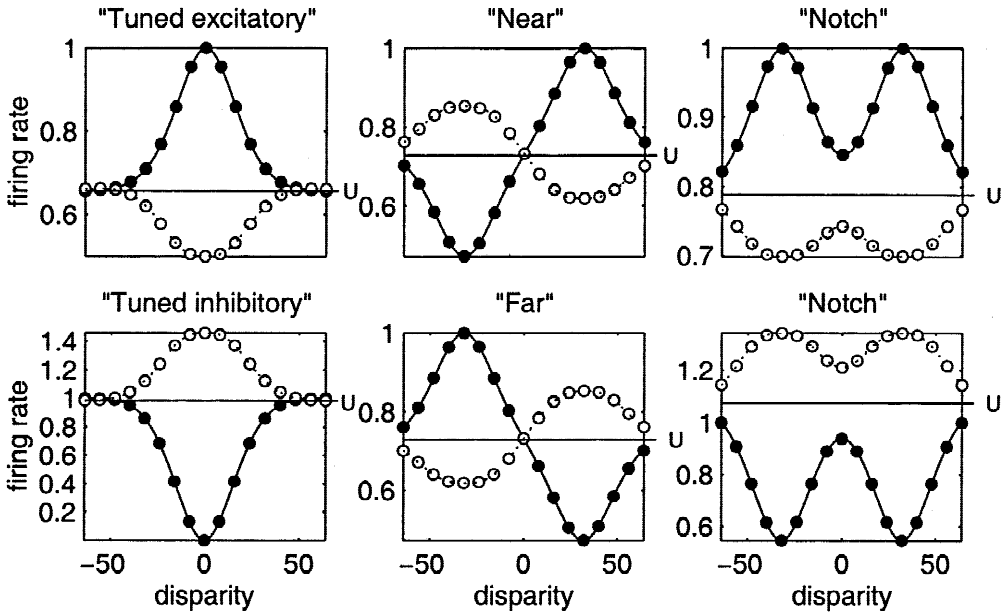

Fig. 10. Our new model with Gaussian RFs (shown in Fig. 11). The six types of disparity tuning curves were obtained as explained in eqns. (19)–(21).

with an ODF-like model in which binocular combination is linear (see Appendix C).

The disparity-modulated component of the tuning curve still follows eqns. (19)–(21), but now every $\mathrm{Pos}(x)$ is replaced by $\mathrm{Pos}(x-\theta)$. Once again, the tuning curve has a constant component that represents the response to uncorrelated stimuli, although the magnitude of this constant is affected by the threshold. By choosing a high enough value for the threshold, we can obtain almost arbitrarily small amplitude ratios. An example is shown in Fig. 12. With the Gabor RFs shown here, the near/far cells retain some anticorrelated response even with the present high threshold. With Gaussian RFs and a similarly high threshold (not shown), none of the cell types show any modulation for anticorrelated stimuli.

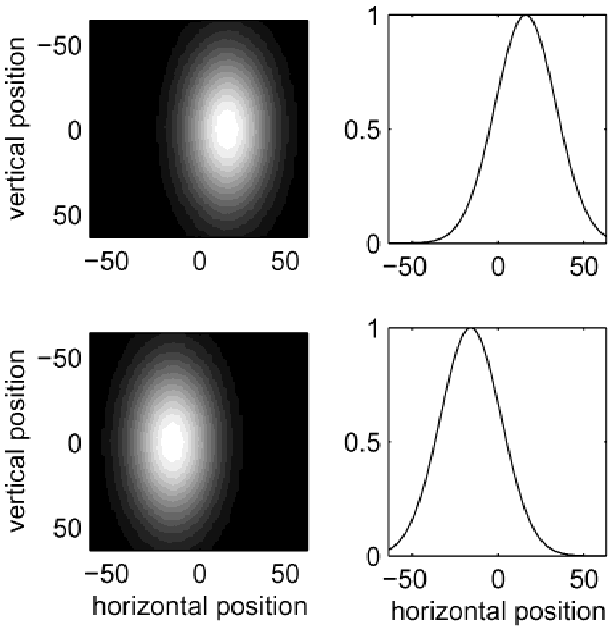

Fig. 11. Receptive fields used in obtaining the disparity tuning curves shown in Fig. 10. The left-hand images show the full RFs as a function of position in the retina. The plots on the right show a horizontal cross section through the RF profiles. The position disparity is 16 pixels. In obtaining the TE/TI even tuning curves (left-most plots of Fig. 10), the upper RF profile was assigned to $\rho^{(1s)}$ and $\rho^{(1d)}$, and the lower to $\rho^{(2s)}$ and $\rho^{(2d)}$. In obtaining the odd and "notch" tuning curves (middle- and right-most plots of Fig. 10), the upper RF profile was assigned to $\rho^{(1s)}$ and $\rho^{(2d)}$, and the lower to $\rho^{(2s)}$ and $\rho^{(1d)}$.

We take this opportunity to explain the unorthodox choice of phases for the Gabor RFs (Fig. 9). The ODF model has the special property that its response depends only on the phase-disparity between left and right RFs, not on the phases themselves. Thus, previous workers have restricted themselves to RFs which are purely odd or purely even, with no loss of generality, even though many physiological cells have RFs with intermediate phases. This property is not true of general models. The response of our modified model depends, in general, on the phase of the RFs in each retina, even for a given phase-disparity. The results shown here were obtained using RFs with a phase of $\pm\pi/4$ (Fig. 9). These produce an amplitude ratio of around 0.9 with a threshold of zero (Fig. 8), and 0.2 with the higher threshold used in Fig. 12. If we used RFs with a phase of 0 in one eye and $\pi/2$ in the other, we would obtain an amplitude ratio of exactly 1, no matter how high we raised the threshold. This property is extremely general: it can be shown (Appendix B) that, for *any* model built from convolutions of the images with RFs, even incorporating monocular nonlinearities which are different in the two eyes, the combination of a purely odd RF in one eye with a purely even RF in the other eye must produce an amplitude ratio of 1.

Complex cells summing many simple cells

The ODF model predicts that the disparity tuning curve should undergo a phase shift of π when the stimulus is anticorrelated. Experimentally, although many complex cells do indeed show

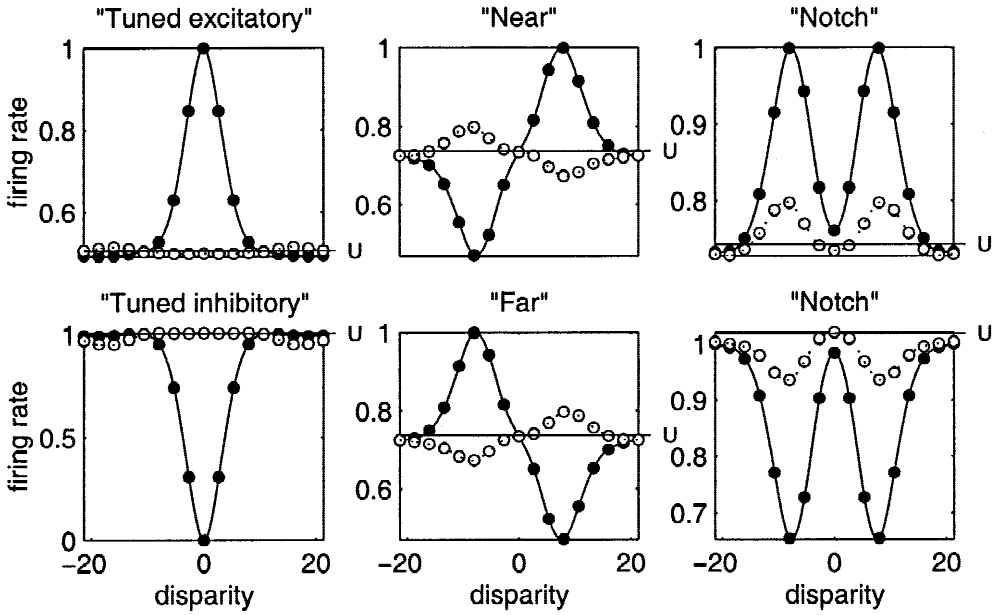

Fig. 12. Our modified model with threshold. The monocular simple cell RFs employed are Gabors, shown in Fig. 9. The monocular simple cells had a high threshold, such that they fired in response to only around 1% of images. The tuning curves shown here represent the mean response to 500,000 stereograms.

phase differences close to π, others clearly do not (Cumming & Parker, 1997). We can combine model tuning curves with significant amplitude attenuation to obtain new complex cells that will exhibit intermediate phase differences. One example is shown in Fig. 13. Even and odd versions of our model, incorporating a high threshold, were used to obtain the first two plots. The third plot shows the sum of the even and odd curves. The result is an even tuning curve for correlated stimuli, and a odd-symmetric curve for anticorrelated stimuli. The circuitry is plausible: it assumes only that several subunits feed onto the same complex cell, an extension of the energy model already proposed by several workers (Zhu & Qian, 1996; Fleet et al., 1996; Qian & Zhu, 1997).

Our model also retains an important property of the original energy model. With a combination of many subunits, whose RFs have the same phase-disparity but random overall phases, the response to drifting gratings is not modulated, as observed experimentally for complex cells.

Behavior of BS cells constructed from monocular simple cells

We have envisaged our model complex cell as receiving input from BS cells in which the combination of inputs from the two eyes is nonlinear [eqn. (22)], owing to a half-wave rectification before summation. Although there are some clear examples in the literature of simple cells whose properties are hard to reconcile with anything other than a linear binocular combination (Ohzawa & Freeman, 1986), other simple cells may show nonlinearities of the form we propose. In fact, it is not critical to our model of complex cells that the postulated BS cells should actually exist as individual neurons in the brain—a complex cell with the properties described by our model could conceivably be built with input directly from monocular simple cells or from the LGN, with the necessary nonlinear combination being achieved at the dendritic level. If they do exist, however, the proposed BS

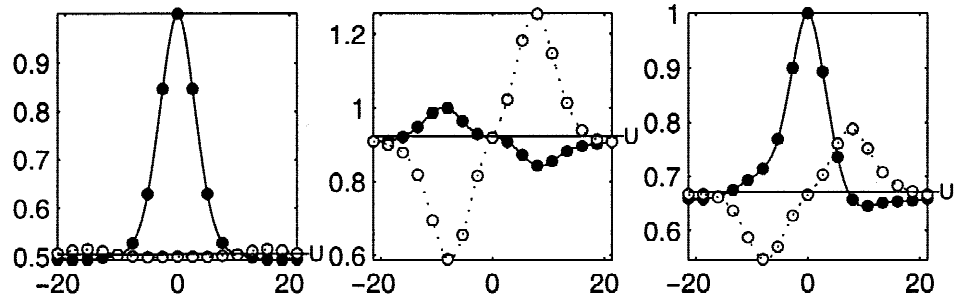

Fig. 13. The left plot shows results from the TE-type model shown in Fig. 12. The middle plot shows results from a far-type model similar to that shown in Fig. 12, except that the model has been adapted to fire more to anticorrelated than to correlated stimuli, by changing the sign of the right-eye convolution wherever it occurred in eqn. (20). The right-most plot shows the sum of the previous two plots, representing a complex cell receiving input from ten BS cells. Other details are as in Fig. 12.

cells would have a number of interesting properties, which we consider here.

Fig. 14 shows the responses of various model simple cells to disparate drifting sinusoidal gratings. The phase difference between the left- and right-eye gratings varies from 0 deg to 330 deg in 30-deg steps, as indicated to the left of each row. The different columns show results for different model simple cells: the ODF binocularly linear simple cell on the left, and then two of our modified simple cells, in which the nonlinearity occurs before binocular combination:

$$S = [\mathrm{Pos}(v_L^{(s)} + v_R^{(d)})]^2,$$

$$S' = [\mathrm{Pos}\{\mathrm{Pos}(v_L^{(s)}) - \mathrm{Pos}(v_R^{(d)})\}]^2,$$

$$S' = [\mathrm{Pos}(v_L^{(s)} + \mathrm{Pos}(v_R^{(d)})]^2. \qquad (23)$$

Column 2 in Fig. 14 shows model simple cells which receive excitatory input from one eye and inhibitory from the other. These were postulated in order to explain the existence of complex cells with odd disparity tuning curves and attenuated response to anticorrelated stimuli. Such a model can explain the existence of cells that show no response to monocular stimulation in one of the two eyes, but are nevertheless sensitive to the interocular phase difference. The model simple cell shown in column 2, for example, clearly responds to stimulation in the right eye only if the stimulation in the left eye exceeds some threshold. If the left eye is shown a gray screen and the right eye a drifting grating, the neuron does not fire at all, whereas with binocular gratings it is sensitive to interocular phase (Fig. 14). It is common to find disparity-selective neurons that appear to have only monocular responses when each eye is tested separately (Ohzawa & Freeman, 1986). By itself, this observation might be explained by a high threshold applied after binocular combination. However, in some examples

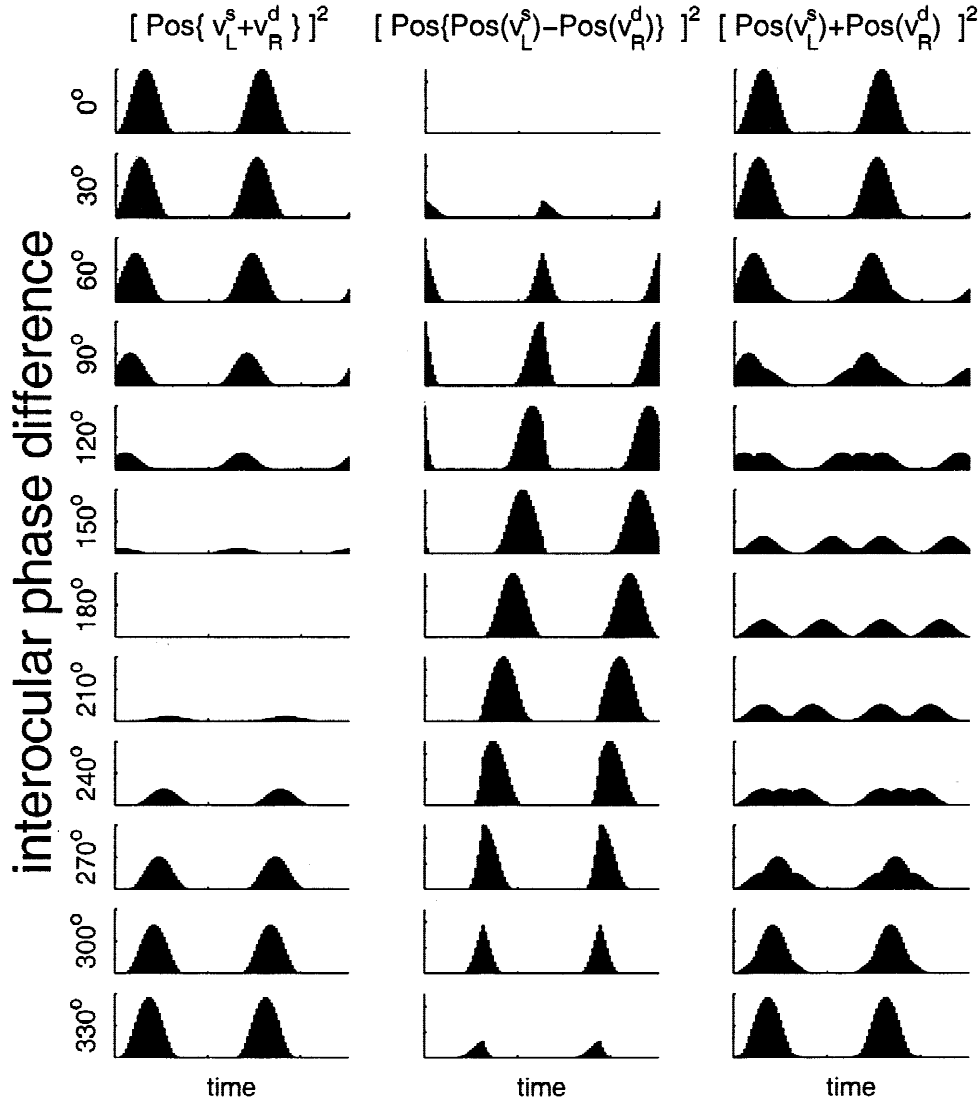

Fig. 14. Responses of model simple cells to drifting sinusoidal gratings. The different columns are for different models, as specified in eqn. (23), with Gabor RFs. The phase of the right eye's grating at time $t = 0$ was the same in every row; the initial phase of the left eye's grating (the interocular phase difference) is indicated to the left of each row. The response is shown over two temporal periods of the stimulus.

(see Prince et al., 2002*b*, Fig. 4c and Discussion) comparison of binocular and monocular responses indicates that the result of stimulation in one eye is always suppressive. This indicates that the output of the monocular RF is passed through an inhibitory synapse *after* half-wave rectification, exactly as occurs in the new model.

Column 3 in Fig. 14 shows the behavior of model simple cells receiving excitatory, half-wave rectified input from both eyes. Such cells are used in our models of both even- and odd-symmetric complex cells. They show characteristic changes in the pattern of response modulation when presented with drifting sinusoidal gratings of different disparities. Although the F_1 response of such a cell is generally similar to that of the ODF linear-combination model, its F_2 response (at twice the grating frequency) is clearly very different. For a particular interocular phase difference, its response is a full-wave rectified sinusoid, rather than the half-wave rectified sinusoid predicted by the linear-combination model. This occurs when the phase difference between the gratings is such that the convolutions with the RFs in each eye are equal and opposite. In the linear-combination model, left- and right-eye contributions cancel out to give a null response. In our model, one eye at a time contributes, giving the frequency-doubling to a drifting grating. This very striking disparity-dependent frequency-doubling has not, to our knowledge, been previously reported.

Detecting a nonlinearity prior to binocular combination

We reexamined data from 117 disparity tuned neurons from V1 of awake monkeys, tested with drifting gratings at multiple disparities (Cumming & Parker, 2000). Of these, 38 neurons were classified as simple on the basis that the $F_1 : F_0$ ratio exceeded 1 for at least one disparity tested.

Fig. 15 shows sample data from one example. At IOP = 0 (upper plot), the cell displays typical simple cell behavior, responding with one burst of spikes in every period of the stimulus. But when the IOP is half a cycle (lower plot), the cell responds with two bursts of spikes for each stimulus period. Fig. 16 shows data from three of our 38 simple cells which showed clear evidence of modulation at the second harmonic of the temporal frequency. Furthermore, a clear progression is observed between modulation at the fundamental frequency and modulation at the second harmonic, as interocular phase alters. These neurons behave more like our model frequency-doubling cells (Fig. 14, column 2) than the ODF simple cell (column 1). For 13 of these 38 cells (34%), the ratio of the response at the second harmonic to the response at the fundamental frequency, $F_2 : F_1$, was greater than 1 at the disparity where the F_1 response was minimal. This is exactly what is predicted by our model, whereas for the ODF model, and a set of generalizations of it which retain the property of linear binoc-

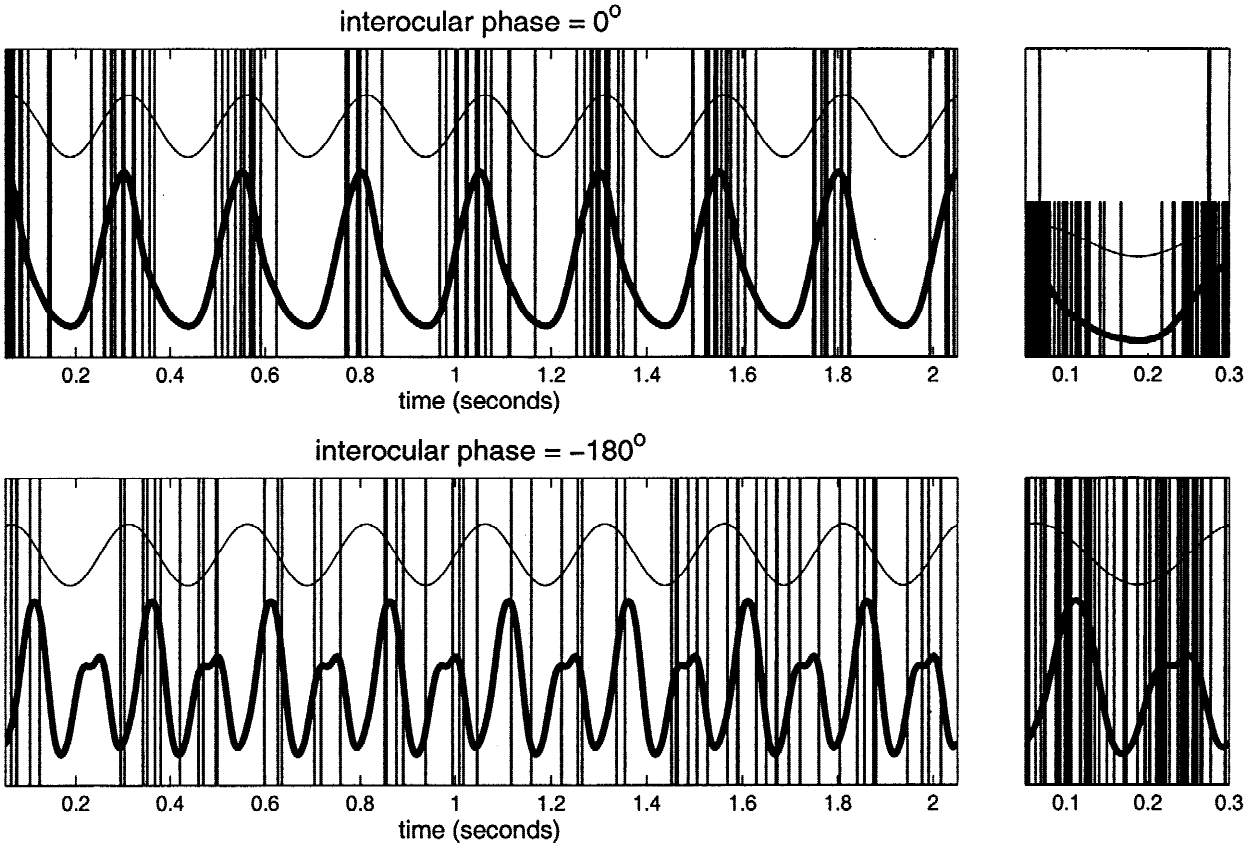

Fig. 15. Cell hg136.0. The monkey was viewing sinusoidal gratings with a spatial frequency of 1 cycle/deg at an orientation of 60 deg to the horizontal, drifting at a rate of 4 cycles/sec. This figure shows results from two stimulus presentations, at IOP of zero (top plots) and half a cycle (a disparity of −0.58, deg lower plots). The long plots on the left show all the spikes recorded during a 2-s window beginning 50 ms after the presentation of the stimulus. The superimposed sine wave (thin line) shows the temporal frequency of the stimulus. The heavier line below shows the estimated firing rate reconstructed from the spike density function obtained after folding all spikes back into one stimulus temporal period (right-hand plots).

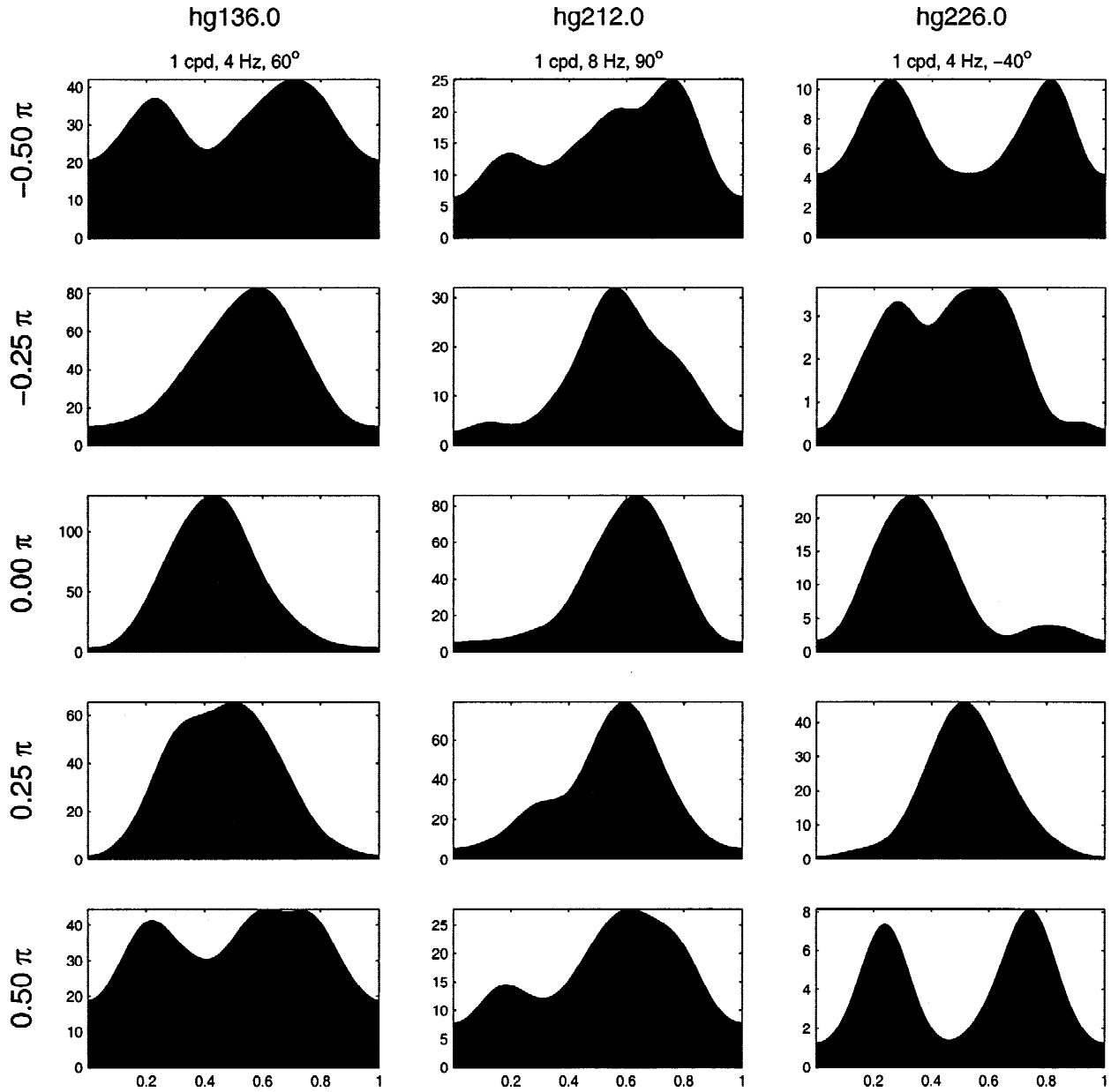

Fig. 16. The columns show the response of three different simple cells to drifting gratings. The first column is for the same cell as in Fig. 15. Each row shows the spike density function for a different interocular phase (indicated to the left of each row), as a function of time (in units of the stimulus temporal period). The drifting gratings are described, at the top of each column, by their spatial frequency, in cycles per degree, temporal frequency, in cycles per second, and orientation, in degrees to the horizontal. The axes are scaled differently in each panel, since the frequency-doubling generally occurs for the lowest firing rates, and so otherwise would be obscured.

ular combination, $F_2 : F_1$ can never exceed 1 (Appendix C). A detailed statistical evaluation of the significance of this finding is made difficult by several factors. First, the data were not collected with this question in mind. Larger numbers of repetitions would be desirable for estimating the temporal modulation in the response. The need for extensive data is exacerbated by the fact that the model predicts the greatest F_2 modulation for the disparity that produces the weakest response. Second, quantitative estimation is complicated by fixational eye movements which occur in the awake monkey. Finally, the predictions of the ODF model depend on the size of the threshold that is applied after binocular combination (Appendix C), so it is not easy to formulate an appropriate null hypothesis. Applying a threshold after binocular summation will also reduce the observed $F_2 : F_1$ ratio for our model neuron, so that there are circumstances in which $F_2 : F_1$ never exceeds 1, even for simple cells constructed in accordance with our model. Nonetheless, at least some BS cells behave as if they receive input from monocular simple cells which themselves have output nonlinearities.

Discussion

The otherwise successful energy model of complex cells fails to explain the response of all V1 neurons to anticorrelated random-dot stimuli (AC-RDS). Most of these cells show amplitude ratios

less than 1, whereas the energy model predicts an amplitude ratio of exactly 1. We show that a simple modification of the model—which may be interpreted as constructing BS cells from the outputs of monocular simple cells—reproduces the behavior of those cortical neurons which are incompatible with the energy model. Of course, the energy model may still be valid for those cells which show amplitude ratios of 1. V1 may contain a mixture of energy-model units and units of the form proposed here. According to this hypothesis, neurons showing strong evidence of linear binocular combination should always have amplitude ratios close to 1. This has yet to be examined experimentally.

Anti-correlated stimuli, which do not support depth perception, are of special interest because of the insight they provide into the solution of the correspondence problem (Cumming & Parker, 1997; Read & Eagle, 2000). They contain many false, local matches, but the visual systems of humans and monkeys are unable to discover any global solution. For human observers, anticorrelated stereograms do not result in a segregated depth percept in which "cyclopean form" (Julesz, 1971) can be perceived. By comparison, any of the machine-vision systems that are capable of solving the correspondence problem in normal correlated stereograms (Dev, 1975; Marr & Poggio, 1979; Pollard et al., 1985) could be trivially modified so that they would then be successful with anticorrelated stereograms.

If V1 complex cells respond only to a global solution, as proposed by Poggio and Poggio (1984), these neurons should not respond at all to AC-RDS. Conversely, the disparity energy model (Ohzawa et al., 1990) predicts that local matches in AC-RDS will evoke disparity tuning of the same amplitude but inverted phase compared with correlated stimuli. Neither of these predictions is borne out. Complex cells do show disparity tuning for AC-RDS, but with reduced amplitude (Cumming & Parker, 1997; Ohzawa et al., 1997). With a completely separate experimental approach, Neri et al. (1999) found that disparity-specific psychophysical "filters" derived from human observers also show an attenuated response for anticorrelated stimuli.

Although Cumming and Parker (1997) argued that the disparity tuning observed with AC-RDS indicates that the complex cells are driven primarily by local features, the reduced amplitude could be taken as evidence that these V1 neurons are somehow sensitive to the presence of a global solution (Ohzawa, 1998), and are hence affected by depth perception. The fact that attenuated anticorrelated response is also observed in anesthetized animals (Ohzawa et al., 1990, 1997) does not in itself argue against top–down feedback (as suggested by Ohzawa, 1998), because if we do not know where or how global stereo matching occurs, we cannot be sure that it would be abolished by anesthesia.

A more serious objection to a top–down mechanism arises from the response to binocularly anticorrelated single bar stimuli. At the neuronal level, these stimuli give a reduced response, which is often phase-inverted (Ohzawa et al., 1990, 1997). Psychophysically, anticorrelated bars produce veridical depth perception in humans (Helmholtz, 1909; Cogan et al., 1995; Cumming et al., 1998); in other words, a disparity that is geometrically signaling depths nearer than the fixation point continues to do so when the bar stimulus is anticorrelated. For these bar stimuli, the implication is that there is a satisfactory global solution of the correspondence problem. It is hard to see how a properly conceived, top–down mechanism can be invoked to explain the attenuated response of V1 neurons to both anticorrelated bars and RDS, when the perceptual experience is so different in the two cases.

Quite separately, Cumming and Parker (2000) have provided further evidence that the activity of V1 complex cells is not affected by global matching. They used sine-wave grating stimuli presented within circular apertures, chosen to be larger than the RF. If the stimuli are displaced by one spatial period of the grating, the portion of the image within the RF is unchanged, but the disparity of the aperture means that the depth of the stimulus is unambiguous. Cells' responses depended essentially only on the stimulus within their RF, arguing against feedback from higher areas. Thus, there are now several converging lines of evidence to suggest that binocular responses of V1 neurons are primarily accounted for by the local anatomical connections within V1.

The present work strengthens this conclusion. We demonstrate that a straightforward modification of the energy model can account for the response of V1 complex cells to both correlated or anticorrelated stimuli. This physiologically plausible, purely local model can produce disparity tuning curves of every observed phase, including those in which anticorrelation introduces a phase change other than π, which exhibit reduced amplitude for anticorrelated stimuli.

Acknowledgments

J.C.A. Read was supported by a Wellcome Trust Training Fellowship in Mathematical Biology. B.G. Cumming was supported by a Royal Society University Research Fellowship. Work in A.J. Parker's laboratory is supported by a Programme Grant from the Wellcome Trust.

References

Adelson, E.H. & Bergen, J.R. (1985). Spatiotemporal energy models for the perception of motion. *Journal of the Optical Society of America A* **2**, 284–299.

Anzai, A., Ohzawa, I. & Freeman, R.D. (1999*a*). Neural mechanisms for encoding binocular disparity: Receptive field position versus phase. *Journal of Neurophysiology* **82**, 874–890.

Anzai, A., Ohzawa, I. & Freeman, R.D. (1999*b*). Neural mechanisms for processing binocular information: I. Simple cells. *Journal of Neurophysiology* **82**, 891–908.

Anzai, A., Ohzawa, I. & Freeman, R.D. (1999*c*). Neural mechanisms for processing binocular information: II. Complex cells. *Journal of Neurophysiology* **82**, 909–924.

Barlow, H.B., Blakemore, C. & Pettigrew, J.D. (1967). The neural mechanisms of binocular depth discrimination. *Journal of Physiology* (London) **193**, 327–342.

Cogan, A.I., Kontsevich, L.L., Lomakin, A.J., Halpern, D.L. & Blake, R. (1995). Binocular disparity processing with opposite-contrast stimuli. *Perception* **24**, 33–47.

Cumming, B.G. & DeAngelis, G.C. (2001). The physiology of stereopsis. *Annual Review of Neuroscience* **24**, 203–238

Cumming, B.G. & Parker, A.J. (1997). Responses of primary visual cortical neurons to binocular disparity without depth perception. *Nature* **389**, 280–283.

Cumming, B.G. & Parker, A.J. (2000). Local disparity not perceived depth is signaled by binocular neurons in cortical area V1 of the macaque. *Journal of Neuroscience* **20**, 4758–4767.

Cumming, B.G., Shapiro, S.E. & Parker, A.J. (1998). Disparity detection in anti-correlated stereograms. *Perception* **27**, 1367–1377.

Dev, P. (1975). Perception of depth in random-dot stereograms: A neural model. *International Journal of Man–Machine Studies* **7**, 511–528.

Fleet, D.J., Wagner, H. & Heeger, D.J. (1996). Neural encoding of binocular disparity: Energy models, position shifts and phase shifts. *Vision Research* **36**, 1839–1857.

Helmholtz, H. von (1909). *Handbuch der physiologischen Optik*. Hamburg, Germany: Voss.

Hubel, D.H. & Wiesel, T.N. (1962). Receptive fields, binocular interaction and functional architecture in the cat's visual cortex. *Journal of Physiology* (London) **160**, 106–154.

Julesz, B. (1971). *Foundations of Cyclopean Perception*. Chicago, Illinois: University of Chicago Press.

Lippert, J. & Wagner, H. (2001). A threshold explains modulation of neural responses to opposite-contrast stereograms. *Neuroreport* **12**, 3205–3208.

Marr, D. & Poggio, T. (1979). A computational theory of human stereo vision. *Proceedings of the Royal Society B* (London) **204**, 301–328.
Movshon, J., Thompson, I. & Tolhurst, D.J. (1978). Spatial summation in the receptive fields of simple cells in the cat's striate cortex. *Journal of Physiology* (London) **283**, 53–77.
Neri, P., Parker, A.J. & Blakemore, C. (1999). Probing the human stereoscopic system with reverse correlation. *Nature* **401**, 695–698.
Nieder, A. & Wagner, H. (2000). Horizontal-disparity tuning of neurons in the visual forebrain of the behaving barn owl. *Journal of Neurophysiology* **83**, 2967–2979.
Nikara, T., Bishop, P.O. & Pettigrew, J.D. (1968). Analysis of retinal correspondence by studying receptive fields of binocular single units in cat striate cortex. *Experimental Brain Research* **6**, 353–372.
Ohzawa, I. (1998). Mechanisms of stereoscopic vision: The disparity energy model. *Current Opinion in Neurobiology* **8**, 509–515.
Ohzawa, I. & Freeman, R.D. (1986). The binocular organization of simple cells in the cat's visual cortex. *Journal of Neurophysiology* **56**, 221–242.
Ohzawa, I., DeAngelis, G. & Freeman, R.D. (1990). Stereoscopic depth discrimination in the visual cortex: Neurons ideally suited as disparity detectors. *Science* **249**, 1037–1041.
Ohzawa, I., DeAngelis, G. & Freeman, R.D. (1997). Encoding of binocular disparity by complex cells in the cat's visual cortex. *Journal of Neurophysiology* **77**, 2879–2909.
Poggio, G.F. & Fischer, B. (1977). Binocular interaction and depth sensitivity of striate and prestriate cortex of behaving rhesus monkey. *Journal of Neurophysiology* **40**, 1392–1405.
Poggio, G.F. & Poggio, T. (1984). The analysis of stereopsis. *Annual Review of Neuroscience* **7**, 379–412.
Poggio, G.F., Motter, B.C., Squatrito, S. & Trotter, Y. (1985). Responses of neurons in visual cortex (V1 and V2) of the alert macaque to dynamic random-dot stereograms. *Vision Research* **25**, 397–406.
Pollard, S.B., Mayhew, J.E.W. & Frisby, J.P. (1985). PMF: A stereo correspondence algorithm using a disparity gradient limit. *Perception* **14**, 449–470.
Prince, S.J.D., Pointon, A.D., Cumming, B.G. & Parker, A.J. (2002*a*). Quantitative analysis of the responses of V1 neurons to horizontal disparity in dynamic random dot stereograms. *Journal of Neurophysiology*, **87**, 191–208.
Prince, S.J.D., Cumming, B.G. & Parker, A.J. (2002*b*). Range and mechanism of encoding of horizontal disparity in macaque V1. *Journal of Neurophysiology*, **87**, 209–221.
Qian, N. & Zhu, Y. (1997). Physiological computation of binocular disparity. *Vision Research* **37**, 1811–1827.
Read, J.C.A. & Eagle, R.A. (2000). Reversed stereo depth and motion direction with anti-correlated stimuli. *Vision Research* **40**, 3345–3358.
Zhu, Y. & Qian, N. (1996). Binocular receptive fields, disparity tuning, and characteristic disparity. *Neural Computation* **8**, 1647–1677.

Appendices

A: Symmetry of convolution products with even-/odd-symmetric RFs

In the basic Ohzawa-DeAngelis-Freeman (ODF) energy model, convolutions from the left and right eyes are added, then squared. The squaring results in two terms involving one eye only, plus one cross-term in which contributions from the left and right eyes are multiplied together. On average, the sum of the monocular convolutions cannot depend either on the disparity between the two retinal images, or on their correlation. It is the cross-term that contains any dependence on binocular disparity.

In this appendix, we consider the situation where the receptive-field (RF) functions possess pure even or odd symmetry about a point in the retina. We prove that if one is even and the other is odd, the disparity tuning curve is odd (see Results, p. 736). It is also easy to show that if both RFs are even, or both odd, then the product of their convolutions yields an even disparity tuning curve. For convenience, we assume that all RFs are symmetric about the retinal position zero. Relaxing this assumption simply shifts the central disparity δ_0 of the tuning curve.

The convolution of a retinal image with an RF was defined in eqn. (3). We now average the product of left and right convolutions over many randomly generated binocularly correlated image pairs, all with disparity δ. We use angle brackets to represent this ensemble averaging. The mean value obtained depends on the disparity. For example, where the left RF has even symmetry and the right odd, the mean convolution product is

$$\langle v_L^{\text{even}} v_R^{\text{odd}} \rangle(\delta) = \left\langle \iint \mathrm{d}x\,\mathrm{d}y\, I_L(x,y)\rho^{\text{even}}(x,y) \times \iint \mathrm{d}x'\mathrm{d}y' I_R(x',y')\rho^{\text{odd}}(x',y') \right\rangle. \quad \text{(A1)}$$

Now, since the right-eye image is a shifted version of the left, we can write $I_R(x,y) = I_L(x+\delta, y)$. Substituting this into the expression for the convolutions, eqn. (A1) and taking the ensemble averaging within the integration over position, we obtain

$$\langle v_L^{\text{even}} v_R^{\text{odd}} \rangle(\delta) = \iint \mathrm{d}x\,\mathrm{d}y \iint \mathrm{d}x'\mathrm{d}y' \langle I_L(x,y) I_L(x'+\delta, y') \rangle \times \rho^{\text{even}}(x,y)\rho^{\text{odd}}(x',y'). \quad \text{(A2)}$$

$\langle I_L(x,y) I_L(x'+\delta,y')\rangle$ is the average value of the product of the contrasts at positions (x,y) and $(x'+\delta, y')$ in the retina. For *spatially invariant* image ensembles, as generally used in experiments (Cumming & Parker, 1997; Poggio et al., 1985), this does not depend on the actual positions in the retinas, only on the distance between them. It is therefore a function—say, $\mathcal{L}$—of two variables: $\mathcal{L}(x - x' - \delta, y - y')$. Furthermore, since the order cannot matter, it must be even in both variables. For example, $\mathcal{L}(x - x' - \delta, y - y') = \mathcal{L}(-x + x' + \delta, y - y')$. So, we now have

$$\langle v_L^{\text{even}} v_R^{\text{odd}} \rangle(\delta) = \iint \mathrm{d}x\,\mathrm{d}y \iint \mathrm{d}x'\mathrm{d}y' \mathcal{L}(x - x' - \delta, y - y') \times \rho^{\text{even}}(x,y)\rho^{\text{odd}}(x',y'). \quad \text{(A3)}$$

Now consider the case where we present image pairs with the opposite disparity, $-\delta$. The expected value of the convolution product is now

$$\langle v_L^{\text{even}} v_R^{\text{odd}} \rangle(-\delta) = \iint \mathrm{d}x\,\mathrm{d}y \iint \mathrm{d}x'\mathrm{d}y' \mathcal{L}(x - x' + \delta, y - y') \times \rho^{\text{even}}(x,y)\rho^{\text{odd}}(x',y'). \quad \text{(A4)}$$

Transforming the dummy integration variables $x \to -x, x' \to x'$ makes no difference, so we can write

$$\langle v_L^{\text{even}} v_R^{\text{odd}} \rangle(-\delta) = \iint \mathrm{d}x\,\mathrm{d}y \iint \mathrm{d}x'\mathrm{d}y' \mathcal{L}(-x + x' + \delta, y - y') \times \rho^{\text{even}}(-x,y)\rho^{\text{odd}}(-x',y'). \quad \text{(A5)}$$

Now using the stated symmetry of the RFs and of the function $\mathcal{L}$, we find that

$$\langle v_L^{\text{even}} v_R^{\text{odd}} \rangle(-\delta) = \iint \mathrm{d}x\,\mathrm{d}y \iint \mathrm{d}x'\mathrm{d}y' \mathcal{L}(x + x' - \delta, y - y') \times \rho^{\text{even}}(x,y)\rho^{\text{odd}}(x',y') = -\langle v_L^{\text{even}} v_R^{\text{odd}} \rangle(\delta). \quad \text{(A6)}$$

Thus, the product $\langle v_L^{\text{even}} v_R^{\text{odd}} \rangle$ is an odd function of disparity.

Precisely analogous manipulations show that, if left and right RFs are both even, or both odd, then the convolution product is an even function of disparity. Note that, in contrast to the *LR* symmetry discussed in the Results, none of these results require the RFs in different eyes to be related in any way. They must simply be individually either even or odd, as indicated. General RFs may be handled by expressing them as a sum of an even and an odd component. (Note that the results may not always be interesting. For instance, if the left and right RFs have spatial periods

separated by many times their bandwidth, they will effectively see uncorrelated images. In this case, the convolution product will, on average, be zero. A function which is everywhere zero is both even and odd. Thus the results still hold formally, even though there is no disparity tuning.)

B: Even-/odd-symmetric RFs always yield amplitude ratios of 1

We consider a very general model, built from a combination of binocular subunits whose output depends only on the convolution of the image with the RF in each eye:

$$C = \sum_j f_j(v_L^{(sj)}, v_R^{(dj)}), \tag{B1}$$

where the f_j are arbitrary functions of two variables. The ODF model is a special case of this class, but so is our modified model which includes nonlinearities prior to binocular combination.

In this appendix, we shall show that if within each subunit j, one eye's RF has pure even symmetry and the other has pure odd symmetry about some point on the retina, then the effect of anticorrelation is simply to reflect the disparity tuning curve about some disparity. It follows that the amplitude ratio is necessarily 1.

To prove this claim, we write the convolutions for one subunit in terms of the Fourier transforms of the images and RFs:

$$v_L^{(s)} = \int_{-\infty}^{\infty} dy \int_{-\infty}^{\infty} dk\, \mathrm{Re}\{\tilde{\rho}^{(s)}(k,y)\tilde{I}^*(k,y)\},$$

$$v_R^{(d)} = \int_{-\infty}^{\infty} dy \int_{-\infty}^{\infty} dk\, \mathrm{Re}\{\tilde{\rho}^{(d)}(k,y)\tilde{I}^*(k,y)e^{ik\delta}\}, \tag{B2}$$

where the tilde represents a one-dimensional Fourier transform along the same axis x along which disparity is applied:

$$\tilde{f}(k,y) = \int_{-\infty}^{\infty} dx\, f(x,y)e^{ikx}, \tag{B3}$$

and we have used the fact that, since the right image is simply the left image displaced through δ along the x axis, $I_R(x,y) = I_L(x-\delta, y)$, then $\tilde{I}_R^*(k,y) = \tilde{I}_L^*(k,y)e^{ik\delta}$.

We shall consider the situation where the left RF is purely even about the origin, and the right RF purely odd about the same point. Then, $\tilde{\rho}^s(k,y)$ is purely real, and $\tilde{\rho}^d(k,y)$ is purely imaginary. Thus,

$$v_L^{(s)} = \int_{-\infty}^{\infty} dy \int_{-\infty}^{\infty} dk \tilde{\rho}^{(s)}(k,y)\,\mathrm{Re}\{\tilde{I}^*(k,y)\},$$

$$v_R^{(d)} = -\int_{-\infty}^{\infty} dy \int_{-\infty}^{\infty} dk \tilde{\rho}^{(d)}(k,y)\,\mathrm{Im}\{\tilde{I}^*(k,y)e^{ik\delta}\}. \tag{B4}$$

Now, consider making three simultaneous manipulations: (1) replace the original stimulus $I(x,y)$ with its mirror image, $I(-x,y)$; (2) present the stimulus at the opposite disparity, $-\delta$; and (3) make the stimulus anticorrelated by contrast inverting the image presented to the right eye. That is, whereas in obtaining eqn. (B4) the left image was $I_L(x)$ and the right image was $I_L(x-\delta)$, we now consider the case where the left image is $I_L(-x)$ and the right image is $-I_L(-x-\delta)$. It turns out that the *same* values are obtained for the convolutions. To see this, note that the Fourier transform of the mirror image is the complex conjugate of that of the original image. But $\mathrm{Re}(z) \equiv \mathrm{Re}(z^*)$, so the left convolution $v_L^{(s)}$ in eqn. (B4) is clearly unchanged. For the right convolution, the term inside curly braces is complex-conjugated with a sign change. But since $\mathrm{Im}(z) \equiv \mathrm{Im}(-z^*)$, once again there is no change to the convolution.

Now, for the random-dot patterns generally used in physiological experiments, any given stimulus $I(x,y)$ is as likely to be presented as its mirror-image $I(-x,y)$. This means that the mean response obtained with anticorrelated patterns at disparity $-\delta$ must be the same as the mean response obtained with correlated patterns at disparity $+\delta$. The effect of anticorrelation is simply to reflect the disparity tuning curve about zero disparity. If we generalize to allow the RFs to be odd- and even-symmetric about arbitrary points in the retina, anticorrelation reflects the disparity tuning curve about a nonzero disparity equal to the position disparity of the RFs. Thus, in order to obtain amplitude ratios less than 1 from any model of this very general type (30), we must avoid pairing pure-even with pure-odd RFs. Phase-disparities of $\pi/2$ are capable of giving amplitude ratios <1, provided that the phase-disparity is not achieved with a phase of $\pi/2$ in one eye and a phase of 0 in the other. This is why, in Fig. 9, the RFs are chosen to have phases of $\pm\pi/4$.

C: Fourier analysis of the response of model simple cells to drifting gratings

We derive the Fourier coefficients characterizing the response, to drifting sinusoidal gratings, of model simple cells in which binocular combination is linear. We consider a binocular simple (BS) cell whose response is given by

$$S = [\mathrm{Pos}(v_L + v_R - \theta)]^P. \tag{C1}$$

This is a generalization of eqn. (4) to include a threshold θ which may be greater than zero, and an arbitrary power P. Note that the nonlinearity is introduced after binocular combination.

The cell is stimulated with drifting sinusoidal gratings:

$$I(x,y,t) = \sin(k_x x + k_y y - \phi + \omega t). \tag{C2}$$

In general, the phase ϕ is different in the two eyes. $\Delta\phi = \phi_L - \phi_R$ is the interocular phase difference. The convolution in eqn. (2) of the grating with the RF is given by

$$v(t) = \mathrm{Im}[\exp(i\omega t - i\phi)\tilde{\rho}], \tag{C3}$$

where $\tilde{\rho}$ is the Fourier coefficient of the RF at the grating frequency:

$$\tilde{\rho} = \iint dx\, dy\, \rho(x,y)\exp(ik_x x + ik_y y) \tag{C4}$$

From eqn. C3, the sum of the left- and right-eye convolutions is

$$v_L(t) + v_R(t) = |R|\sin(\omega t - \arg R), \tag{C5}$$

where

$$R = \exp(i\phi_L)\tilde{\rho}^{(s)} + \exp(i\phi_R)\tilde{\rho}^{(d)},$$

$$|R| = |\tilde{\rho}^{(s)}|^2 + |\tilde{\rho}^{(d)}|^2 + 2|\tilde{\rho}^{(s)}||\tilde{\rho}^{(d)}|\cos(\Delta\phi + \Delta\xi), \tag{C6}$$

where $\Delta\xi$ is the phase disparity between the left and right RFs, that is, the difference in the arguments of the complex quantities $\tilde{\rho}^{(s)}$ and $\tilde{\rho}^{(d)}$. The absolute value of the nth Fourier coefficient of the response to the drifting grating is

$$F_0 = \left| \int_0^{2\pi/\omega} dt S(t) \right|, \qquad F_{n>0} = 2\left| \int_0^{2\pi/\omega} dt \exp(in\omega t)S(t) \right|. \tag{C7}$$

It can be shown that this is given by

$$|F_{n>0}| = 2|R|^P \left| \int_T^{\pi/\omega - T} dt \exp(in\omega t)[\sin(\omega t) - \theta/|R|]^P \right|, \tag{C8}$$

where T is defined to be the smallest value satisfying $\sin(\omega T) = \theta/|R|$. Notice that $|R|$, and hence T, depend on the interocular phase. Eqn. (C8) is valid for interocular phases such that $|R| > \theta$. If $\theta \geq |R|$, the cell does not respond at any stage of the cycle, so all Fourier coefficients are zero. Notice that if the threshold is zero [i.e. half-wave rectification, as originally envisaged by Ohzawa et al. (1990)], so that $T = 0$, then the Fourier coefficients depend on interocular phase only through the overall factor $|R|^P$, and so the *ratio* of any two Fourier coefficients is independent of interocular phase. For the case $\theta = 0$ and $P = 1$, $F_1 : F_0 = \pi/2$, and $F_2 : F_1 = 4/3/\pi$; for $\theta = 0$ and $P = 2$, $F_1 : F_0 = 16/3\pi$, and $F_2 : F_1 = 3\pi/16$. In general, the ratio of any two Fourier coefficients will depend on the interocular phase *via* the ratio $\theta/|R|$. However, when these ratios are calculated numerically, it turns out that $F_1 : F_0$ is always greater than 1, meaning that these cells would be classified as simple according to the classification criterion of Movshon et al. (1978). The ratio $F_2 : F_1$ never exceeds 1. It approaches 1 as $\theta/|R| \rightarrow 1$; this is the limiting case where the threshold suppresses any response in the cell. Thus, frequency-doubling cannot be obtained by any member of this rather wide class of model cells in which binocular combination is linear. This conclusion is independent of the form of the RFs.